

Bjorn Stevens

# Bulk boundary-layer concepts for simplified models of tropical dynamics

Received: 12 August 2005 / Accepted: 2 May 2006  
© Springer-Verlag 2006

**Abstract** We review bulk representations of tropical and subtropical maritime atmospheric boundary layers. Three types of bulk representations are studied in detail: stratocumulus topped mixed layers, trade-wind layers, and sub-cloud mixed layers. Through the development of a consistent description of these disparate regimes, connections among their varied representations are emphasized, as well as their relation to regions of deeper convection. New results relating to the equilibrium mass flux and cloud fraction in the trade winds; the ability of bulk models to represent qualitatively major cloud regimes; and the relationship amongst different bulk representations of the surface layer are presented. Throughout we emphasize the identification of consistent and physically based mixing and cloud regime rules for use in intermediate complexity models of the tropical climate, which in turn can be used to study cloud and dynamical interactions on larger scales.

**Keywords** Atmospheric boundary layer · Entrainment · Cumulus mass flux

**PACS** 92.60.Cc, 92.60.Fm, 92.60.hk, 92.60.Ox, 92.70.Np

## 1 Introduction

Bulk, or integral, models of the atmospheric boundary layer (ABL) have long proven useful in a variety of contexts. Indeed the very definition of the boundary-layer depth in classical theory is in terms of an integral over the depth of a layer [36]. Bulk ABL models have appeared as a basis for parameterizing the ABL in larger-scale models [3, 12], and as essential elements in simple thermodynamic models of the tropical climate system [7, 25]. They are also often used as the basis for diagnostic studies of the ABL [1] and particular processes, or ABL regimes, such as stratocumulus [17, 19, 49], surface winds over the tropical ocean [24, 45], trade-wind cloudiness [5, 6, 29], or deep convection [14, 34]. A seminal study of this framework is one component of the landmark paper by Arakawa and Schubert [3]. The proliferation of such approaches and our deepening understanding of processes embodied by them motivate our current investigation.

In this paper we draw on this rich literature of bulk, or integral, representation of the ABL and attempt to extract those ideas of most relevance to the representation of tropical circulations. Our idea is to provide a unified framework through which varied and sometimes quite specialized ideas can be described, and relationships amongst seemingly disparate lines of thought can be clarified. The hope is that a unified presentation of the mathematical structure of past ideas, and a careful consideration of important (and in some cases novel) limits will make this body of thought both more understandable, and accessible, to the broader scientific community. Although partly a review, a number of novel results emerge, most commonly in the form of simplifying assumptions, or simple limits, which help deepen our physical understanding.

---

Communicated by R. Klein

B. Stevens  
Department of Atmospheric and Oceanic Sciences, UCLA, Los Angeles, CA 90095-1565, USA  
E-mail: bstevens@atmos.ucla.edu

**Table 1** Summary of operators and subscripts, defined relative to a generic field variable  $\phi$ . These operators are mostly discussed in Sect. 2

Symbol	Meaning	Reference
$\bar{\phi}$	The expected value of $\phi$	
$\phi'$	Fluctuations, $\phi' \equiv \phi - \bar{\phi}$	
$\hat{\phi}$	The bulk average of $\phi$ (over $h$ )	
$\phi_+, \phi_-$	Value of $\phi$ just above/below $h$	
$\phi_m$	Sub-cloud layer average	
$\phi_f$	Free tropospheric value	
$\phi_0$	Surface value	
$\phi_\infty$	Stationary state	
$\phi_{00}$	Basic state	
$\Delta_+ \phi$	$\phi_+ - \hat{\phi}$	
$\Delta_0 \phi$	$\hat{\phi} - \phi_0$	
$\Delta_m \phi$	Change in $\phi$ across the sub-cloud layer	e.g., $\Delta_m F$ below (52)
$\Delta \phi$	$\phi_+ - \phi_0$	
$\nabla$	Horizontal divergence operator, $\{\partial_x, \partial_y\}$	Above (3)
$D/Dt$	Material derivative following $\hat{\mathbf{u}}$	(9)

The emphasis of this study is on developing the theory of bulk representation of the thermodynamics structure of the ABL over the ocean, but away from regions of deep convection. Such an emphasis is motivated by the fact that cloud processes in such regions are thought to be critical for climate, and that thermodynamically these regions tend to be most distinct from the free troposphere, and thus more susceptible to neglect. In Sect. 2 we develop the notation used throughout the remainder of the paper. The structure of a generic bulk description of the ABL and its energetics is provided in Sect. 3. Section 4 explores the behavior of the bulk theory under constraints appropriate for regions of stratocumulus. In Sect. 5 two different approaches for representing trade cumulus are presented. Ways of using the ideas developed in Sects. 4 and 5, coupling them to one another, as well as to boundary-layer dynamical processes, and neighboring regions of deep convection are discussed in Sect. 6, as are limitations to the bulk approach. A brief summary and conclusions are presented in Sect. 7.

## 2 Setup and notation

Because the number of symbols in moist thermodynamic systems can be large, and because many of the operations we perform are similar for the different types of boundary layers considered, it proves convenient to establish a consistent notation. This is developed below. For subsequent reference, the results of this section are also summarized in Tables 1 and 2. These tables also contain a complete summary of the symbols which otherwise are introduced as needed.

Throughout we consider the structure of shallow (as compared to an atmospheric scale-height) layers, for which the atmospheric analog to the Boussinesq system (wherein the basic state potential temperature  $\theta_{00}$  rather than actual temperature is constant) provides a good analog to the real fluid. Thus the independent variables are the three components of physical space  $\{x, y, z\}$  and time  $t$ . A less restrictive, but mathematically equivalent, system of equations follows by working in mass coordinates, in which case pressure  $p$  replaces height  $z$  as an independent variable, and mass fluxes replace volume fluxes. Our terminology often anticipates this equivalence by equating volume fluxes with mass fluxes – in the Boussinesq system these are linearly related by the basic state density, which is in any case near unity.

We choose to describe the thermodynamic state of our system in terms of the liquid-water static energy,  $s \equiv c_p T + gz - Lq_l$ , the total-water specific humidity  $q$ , and the pressure  $p$ . Here  $q_l$  is the liquid-water specific humidity,  $c_p$  is the isobaric specific enthalpy,  $L$  is the enthalpy of evaporation, and  $g$  is the gravitational acceleration. Throughout we use an overbar to denote an ensemble-averaged quantity, so the fluctuation of some field variable  $\phi$  is defined as

$$\phi' \equiv \phi - \bar{\phi}. \quad (1)$$

Given the surface pressure,  $p_0$ , the ensemble-averaged pressure is assumed to be hydrostatic,  $\bar{p}(x, y, z, t) = p_0 + \int_0^z \rho_{00} g \, dz$ , where  $\rho_{00}$  denotes a basic state density, which is constant, consistent with a Boussinesq system. Maintaining the hydrostatic variation of pressure through the depth of even a shallow boundary layer is critical for a determination of adiabatic variations in the mean-state temperature and hence cloud properties.

**Table 2** Summary of variables, parameters and constants

Symbol	Meaning	Reference
$c_p$	Isobaric specific enthalpy	1,010 J kg <sup>-1</sup>
$e$	Turbulence kinetic energy	Above (25)
$g$	Gravity	9.81 m s <sup>-1</sup>
$h$	Depth of bulk layer	
$h_*$	Stratocumulus scale depth	(38)
$m_u, m_d$	Up- and downdraft mass fluxes	Above (76)
$p$	Pressure	
$q$	Total-water specific humidity	
$q_l$	Liquid-water specific humidity	
$q_s$	Saturation specific humidity	
$s$	Liquid-water static energy, $s \equiv c_p T + gz - q_l z$	
$\mathbf{u}$	Horizontal velocity $\mathbf{u} = \{u, v\}$	
$w$	Vertical velocity	
$w_*$	Deardorff velocity scale	(30)
$z$	Height above surface	
$z_i$	Height of inversion	
$C$	Bulk exchange coefficient	0.0011 see Sect. 3.1.1
$E$	Entrainment velocity	Sect. 3.1.3
$\tilde{E}$	Effective entrainment velocity	(80)
$K$	Eddy diffusivity	(23)
$M$	Boussinesq mass (volume) flux	Sect. 3.1.2
$N$	Ratio of $\Delta_m F$ to sub-cloud radiative flux divergence	(57)
$N_c$	Brunt-Väisälä frequency, $(g/\theta_{00})d\bar{\theta}_v/dz$	
$R$	Nondimensional cumulus topped boundary layer (CTBL) height	(57)
$R_d, R_v$	Gas constants for dry air and water vapor	287.0, 461.5 J kg <sup>-1</sup> K <sup>-1</sup>
$T$	Temperature	
$T_v$	Virtual temperature	(2)
$V$	Surface exchange velocity	Sect. 3.1.3
$\alpha$	Nondimensional entrainment, $\alpha \equiv E \Delta_{+s} / \Delta F_s$	(34)
$\alpha_B$	Buoyancy flux ratio constraining entrainment	(45)
$\alpha_m$	updraft to downdraft mass flux ratio	Above (76)
$\beta_-$	Mixing fraction for parameterizing cloud-base jump	(48)
$\beta_+$	Mixing fraction for parameterizing cloud-top jump	Above (65)
$\phi$	A generic (usually adiabatic invariant) field variable	Sect. 2
$\gamma$	Ratio of radiative to surface fluxes	(57)
$\eta$	Height of cloud base (lifting condensation level or LCL)	
$\eta_*$	Moisture scale height	(40)
$\kappa$	Entrainment flux ratio $\kappa \equiv -\mathcal{B}_- / \mathcal{B}_0$	Above (30)
$\lambda_{1,2,3}$	Eigenvalues of bulk stratocumulus topped boundary layer (STBL) model	
$\sigma$	Nondimensional stability	(38)
$\sigma_h$	Standard deviation of $h$	
$\epsilon$	Dissipation rate of $e$	Below (25)
$\rho$	Density	
$\theta$	Potential temperature $\theta = T(p_{00}/p)^{R_d/c_p}$	
$\theta_v$	Virtual potential temperature $\theta_v = T_v(p_{00}/p)^{R_d/c_p}$	
$\zeta$	Nondimensional mixing height	(49)
$\Delta$	See Table 1	
$\ell$	Mixing length	Below (23)
$\mathcal{A}$	Cloud fraction	
$\mathcal{B}$	Buoyancy flux	Below (25)
$\mathcal{D}$	Divergence of bulk wind	Below (11)
$\mathcal{D}_*$	Necessary $\mathcal{D}$ for cloud-free solutions	
$\mathcal{L}$	Liquid-water path $\int_0^h \rho_0 q_l dz$	

While very small-scale fluctuations in pressure are the means by which the fluid remains incompressible, they add little to the thermodynamic description of the mean state, or the energetics. Hence, when evaluating the latter it proves sufficient to relate buoyancy fluctuations linearly to fluctuations in the virtual potential temperature,  $\theta_v$ , as

$$b' \equiv -g \frac{\rho'}{\rho_{00}} \approx g \frac{T'_v}{T_{00}} \approx g \frac{\theta'_v}{\theta_{00}} \quad \text{with} \quad T_v \equiv \frac{p}{\rho R_d} = T [1 + 0.608q - 1.608q_l]. \quad (2)$$

The numerical factors account for the difference in gas constants for vapor and air respectively<sup>1</sup>, which arise because the effective gas constant of the ideal fluid depends on the mass fraction of water. The subscript 00 denotes a basic state value. Given the characterization of the state of the system (i.e.,  $s$ ,  $q$  and  $p$ ) in equilibrium all other thermodynamic variables (such as  $\theta_v$ ) are straightforward to calculate. The dynamic state of the system is given by the velocity vector  $(u, v, w)$ . Because one of the motivations for developing a bulk description of the ABL is to integrate out vertical dependencies, we distinguish between vertical and horizontal motion. Thus  $\mathbf{u}$  is reserved for the horizontal velocity, and  $\nabla$  is defined to be a two-dimensional operator in the horizontal plane, i.e.,  $\nabla \equiv \{\partial_x, \partial_y\}$ . With this notation the Boussinesq continuity equation becomes:

$$\nabla \cdot \mathbf{u} + \partial_z w = 0. \quad (3)$$

Both  $s$  and  $q$  are chosen as state variables because, to a degree commensurate with our interest, they are invariant following reversible displacements of a fluid admitting phase changes. To aid the development of equation sets that apply equally to both  $s$  and  $q$ , (or for that matter any adiabatic, scalar, invariant of the flow) hereafter we restrict  $\phi$  to denote a generic adiabatic invariant, i.e., for the most part  $\phi \in \{s, q\}$ .

The depth of the ABL is denoted by  $h$ , and the depth of the sub-cloud layer is measured by  $\eta$  sometimes also called the lifting condensation level (LCL). Because we idealize the fluid in a manner that admits discontinuities in state variables at  $h$  we develop a notation which admits one-sided limits, such that

$$h_{\pm} \equiv \lim_{\epsilon \rightarrow 0} h \pm \epsilon, \quad (4)$$

and,

$$\phi_{\pm} \equiv \overline{\phi}(x, y, t, h_{\pm}) \quad (5)$$

where the subscript  $\pm$  should be interpreted as either plus or minus. Bulk averages are denoted by the carat, such that

$$\widehat{\phi}(x, y, t) \equiv \frac{1}{h_+} \int_0^{h_+} \overline{\phi}(x, y, z, t) dz. \quad (6)$$

Note that for this case, as for the subscript “+” or “−”, the reference to ensemble averages is implicit. Differences between  $\widehat{\phi}$  and values just above  $h$  or at the surface are denoted by

$$\Delta_+ \phi \equiv \phi_+ - \widehat{\phi} \quad \text{and} \quad \Delta_0 \phi \equiv \widehat{\phi} - \phi_0, \quad (7)$$

respectively, and we further define

$$\Delta \phi \equiv \Delta_+ \phi + \Delta_0 \phi. \quad (8)$$

That the  $\Delta$  symbol operates on the ensemble-averaged value of the field is again implicit. In addition, the subscripts  $f, m, 0$  and  $\infty$  are used at times to denote values representative of the free troposphere, the sub-cloud mixed layer, the surface, and the  $t \rightarrow \infty$  (steady-state) solution respectively. Depending on the context  $\phi_f$  may, or may not, equal  $\phi_+$ , likewise  $\phi_m$  may or may not equal  $\widehat{\phi}$ . Note that, in the case when  $h$  is associated with the cloud top,  $\Delta_+ \phi = \phi_f - \widehat{\phi}$ , which is not true in cases when  $h$  is identified with the height of the sub-cloud layer.

To help summarize some of this notation, Fig. 1 shows the structure of a stratocumulus-topped ABL for which  $\widehat{s}/c_p \approx 289$  K, and  $s_f$  varies significantly with height, such that  $s_+/c_p \approx 300$  K,  $\widehat{q} \approx 8.9$  g kg<sup>−1</sup>, and  $q_f$  is approximately constant so that  $q_+ \approx 1.6$  g kg<sup>−1</sup>.  $s_0$  and  $q_0$  are not indicated but correspond to a sea-surface temperature roughly 1–1.5 K warmer than the overlying air. Cloud top is at  $h = 855$  m and  $\eta \approx 580$  m.

Lastly, in anticipation of the development of equation sets valid for the bulk fluid, we define here the substantial derivative with respect to the bulk average of the ensemble-averaged horizontal flow, such that

$$\frac{D}{Dt} \equiv \partial_t + \widehat{\mathbf{u}} \cdot \nabla, \quad (9)$$

where for emphasis it is worth repeating that both  $\mathbf{u}$  and  $\nabla$  are defined over the horizontal plane.

<sup>1</sup>  $(R_v - R_d)/R_d \approx 0.608$ , with  $R_v = 461.5$  J kg<sup>−1</sup> and  $R_d = 287$  J kg<sup>−1</sup> the gas constants for water vapor and dry air respectively.

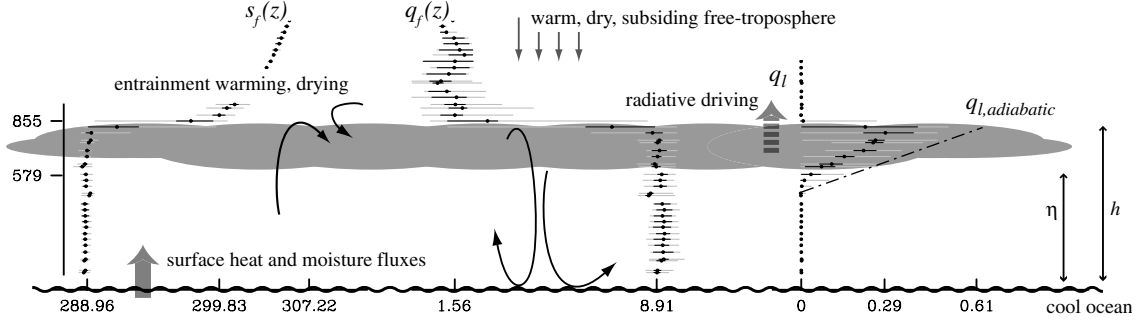


**Fig. 1** Structure of the stratocumulus-topped boundary layer as observed during the first research flight of DYCOMS-II. Here the ordinate shows the height of cloud base and cloud top. In the *leftmost panel* the values of  $\widehat{s}/c_p$ ,  $s_+/c_p$  and  $s/c_p$  at 1,500 m are given on the horizontal axis, similarly for the *middle panel* where values for  $q_+$ , and  $\widehat{q}$  are given. Cloud coverage is near 100% with values of the maximum mean liquid water at any flight level and the adiabatic value also labeled. The main processes contributing to the thermodynamic structure of the layer are indicated schematically. The thermodynamic profiles are constructed from the entirety of the flight data: *gray lines* show range, *black lines* show inter-quartile spread and *dots* show median values

### 3 Bulk theory

In this section we first develop bulk, or vertically averaged, equation sets for a generic variable  $\phi$ . In so doing we show how certain velocity scales are defined as a basis for closing the resultant system of equations. The bulk equations are then explored in reference to a layer of fixed depth in Sect. 3.2. Because it is often used as a basis for closing the bulk system of equations, the bulk energetics of the layer are reviewed in Sect. 3.3. The section concludes with a brief discussion of the relationship between bulk and mixed-layer theory in Sect. 3.4.

#### 3.1 Thermodynamic evolution of a variable depth atmospheric boundary layer

Focusing for a moment on the state variables, a traditional Reynolds decomposition into expected values and fluctuations results in the following equation for the expected values,

$$\partial_t \bar{\phi} + \bar{\mathbf{u}} \cdot \nabla \bar{\phi} + \bar{w} \partial_z \bar{\phi} = -\nabla \cdot \overline{\mathbf{u}'\phi'} - \partial_z \overline{w'\phi'} - \partial_z \bar{F}_\phi. \quad (10)$$

The first two terms on the right-hand side (RHS) describe a turbulent flux, which because of molecular processes acts irreversibly from the perspective of the ensemble-averaged quantities. The last term on the RHS involves  $\bar{F}_\phi$ , the diabatic flux of  $\phi$  not associated with fluid motions, i.e., precipitation or radiative transfer, but not mixing. Its divergence acts as a source of  $\phi$ . To the extent  $\bar{F}_\phi$  depends nonlinearly on the fluid state it will depend on the fluctuating component of the fluid. Equation (10) is the starting point for almost any analysis of the thermodynamics of high Reynolds number fluids.

In the case when (i) the turbulent flux of  $\phi$  is horizontally homogeneous; and (ii) baroclinic circulations within the ABL contribute negligibly to the evolution of  $\widehat{\phi}$  (i.e.,  $\widehat{\mathbf{u}\phi} = \widehat{\mathbf{u}}\widehat{\phi}$ ) the bulk average of (10) is simply

$$h \frac{D\widehat{\phi}}{Dt} - \Delta_+ \phi \left[ \frac{Dh}{Dt} + \mathcal{D}h \right] = -\Delta \overline{w'\phi'} - \Delta F_\phi \quad (11)$$

where  $\mathcal{D} \equiv \nabla \cdot \widehat{\mathbf{u}}$  denotes the divergence of the bulk wind. Integrating the continuity equation (3) over the ABL yields

$$\mathcal{D}h = -\bar{w}_+ + \Delta_+ \mathbf{u} \cdot \nabla h. \quad (12)$$

So  $\mathcal{D}h$  (sometimes referred to as the subsidence, where  $\bar{w}_+$  is defined positive upward) is very nearly equal to the value of the vertical velocity at  $h_+$ . In the limit of  $\Delta_+ \mathbf{u} = 0$ , which is a reasonable one because the velocity jumps at the top of the layer tend to be small, (12) implies that  $\mathcal{D}h \approx -\bar{w}_+$ , which is a common assumption. Note that in deriving (11) and defining  $\mathcal{D}$  it has not been necessary to assume that  $\nabla \cdot \widehat{\mathbf{u}}$  is constant over the layer as is sometimes thought.

For reasons that will become clear shortly we define three velocity scales,  $V$ ,  $M$ , and  $E$ , with positive denoting an upward velocity:

$$V \equiv -\frac{\overline{w'\phi'_0}}{\Delta_0\phi}, \quad M \equiv -\frac{\overline{w'\phi'_+}}{\Delta_+\phi} \quad \text{and} \quad E \equiv \frac{Dh}{Dt} + \mathcal{D}h + M. \quad (13)$$

So doing assumes that  $\overline{w'\phi'_0}$  vanishes with  $\Delta_0\phi$ , and that  $\overline{w'\phi'_+}$  vanishes with  $\Delta_+\phi$ . If we further assume that  $V$  and  $M$  are the same irrespective of whether  $\phi$  is associated with  $s$  or  $q$ , then conservation of mass (volume), enthalpy (as measured by  $\hat{s}$ ), and moisture within the bulk layer follow directly from (11) and (13):

$$\frac{Dh}{Dt} = E - \mathcal{D}h - M \quad (14)$$

$$\frac{D\hat{s}}{Dt} = \frac{E\Delta_+s - V\Delta_0s - \Delta F_s}{h} \quad (15)$$

$$\frac{D\hat{q}}{Dt} = \frac{E\Delta_+q - V\Delta_0q - \Delta F_q}{h}. \quad (16)$$

These three equations are the basis for all consistent integral treatments of the thermodynamic state of the ABL. As written above they involve 14 unknowns:  $h$ ,  $\hat{\mathbf{u}}$ ,  $E$ ,  $M$ ,  $V$ ,  $\hat{s}$ ,  $s_+$ ,  $s_0$ ,  $\overline{F}_s$ ,  $\hat{q}$ ,  $q_+$ ,  $q_0$ ,  $\overline{F}_q$  note that  $\mathcal{D}$  is not among them because  $\hat{\mathbf{u}}$  is given. Hence 11 auxiliary statements are required for closure. By specifying the state of the large-scale atmosphere and ocean (effectively the boundary conditions) one in effect specifies  $\hat{\mathbf{u}}$ ,  $s_0$ ,  $q_0$ ,  $s_+$ ,  $q_+$  and closure only requires models of  $\overline{F}_s$ ,  $\overline{F}_q$ ,  $V$ ,  $M$ , and  $E$ . Typically  $\overline{F}_q$  is associated with precipitation, while  $\overline{F}_s$  will depend on the combined effects of radiation and precipitation. Both processes act non-locally by transporting enthalpy across fluid streamlines. In the subsequent exposition we will mostly consider the non-precipitating limit, i.e.,  $\overline{F}_q = 0$ , in which case  $\overline{F}_s$  only represents the radiative flux divergence across the layer, a process which is relatively well described by our present understanding of radiative transfer given knowledge of the layer's state. The exchange velocities,  $V$ ,  $M$  and  $E$  require more discussion and are treated in turn below.

### 3.1.1 Surface exchange, $V$

From (13),  $V$  defines the surface fluxes. Of the three velocity scales it is the best understood, as both empirically and (at least in certain limits) theoretically, it is well characterized. Given knowledge of, or an assumption about, the structure of  $\overline{\phi}$  within the ABL,  $V$  follows directly from surface-layer similarity. For most practical purposes this theory can be used to define the surface exchange velocity  $V$ :

$$V = C \|\hat{\mathbf{u}}\|, \quad (17)$$

where  $C$  is a dimensionless parameter that depends on the structure and stability of the surface layer [12, 15]. For a reasonably wide range of conditions it may be effectively modeled by a constant. Hereafter we take its value to be 0.0011.

### 3.1.2 The mass flux, $M$

From (13),  $M$  defines the turbulent flux just above the ABL. Many descriptions of the ABL (including ours, with the exception of our discussion in Sect. 5.1) associate  $h$  with the depth of the surface-bounded turbulent layer, in which case the presence of a turbulent flux above the ABL appears paradoxical. However if we define the ABL to be the layer which is globally turbulent, then one can admit patches of turbulence above the ABL. Cumulus clouds, whose active area typically covers a small fraction (2–5%) of the ABL, are good examples of such regions. Typically they are modeled as compact regions (effectively plumes) that transport air out of the ABL at a rate given by  $M$ . From this point of view one can define  $M$  in terms of the tracer flux that the ejected mass transports, and from which (13) follows naturally (although to truly be a mass, rather than volume, flux it should be multiplied by the basic state density). A more formal derivation of (13) as a model for the flux just above the ABL associated with cumulus clouds is given in [39]. Although this justifies the form of the closure in (13) it says nothing about the value of  $M$ . Indeed, how to determine  $M$  is a topic of active research and is discussed in more detail in Sect. 5.2.

### 3.1.3 Entrainment, $E$

Using (12) one can rewrite (14) as

$$(\partial_t + \bar{\mathbf{u}}_+ \cdot \nabla) h_+ = \bar{w}_+ - M + E. \quad (18)$$

This equation states that the change in the height of the interface  $h$ , following its motion, is determined by the flux of fluid into the control volume it bounds (as measured by the average vertical velocity at the interface,  $\bar{w}_+$ , which just integrates the divergence) minus the mass flux out of the volume (in association with cumulus venting and measured by  $M$ ), and  $E$ . It is in this sense that  $E$  represents the *adiabatic* growth rate of the layer, i.e., the rate at which the turbulent ABL deepens by mixing into the overlying fluid. Hence its identification with entrainment. Note that for  $E = 0$  the ABL can still deepen, for instance through local convergence as embodied by  $\bar{w}_+$ .

Another way to look at  $E$  is by integrating (10) between  $h_-$  and  $h_+$ , in which case for  $\phi_- = \hat{\phi}$

$$E = -\frac{\overline{w'\phi'}_- - (\bar{F}_{\phi,+} - \bar{F}_{\phi,-})}{\phi_+ - \phi_-} \approx -\frac{\overline{w'\phi'}_-}{\Delta_+\phi}, \quad (19)$$

where the latter equality follows in the case where  $\hat{\phi} = \phi_-$  and  $F$  is continuous across the interface. In some cases this second approximation is not appropriate [27]; nonetheless, it serves to place  $E$  in a context similar to  $M$  and  $V$ , as a model for an inter-facial flux, which in this case is called the entrainment flux. Differences between  $E$  and  $M$  determine the evolution of the strength of the contact discontinuity at  $h$ , i.e.,  $\partial_t \Delta_+\phi$ .

### 3.2 Fixed boundary-layer depth

In lieu of defining a mass budget for the ABL, and directly modeling the exchanges of mass, enthalpy (heat) and moisture between the ABL and its environment, it often proves convenient simply to define the ABL as a layer of fixed depth. Typically this may be associated with the lowest model level. In this case, integrating (10) over the specified layer results in an equation for its evolution which is identical to (11) without terms involving variations in  $h$ ,

$$h \frac{D\hat{\phi}}{Dt} - \Delta_+\phi \mathcal{D}h = -\Delta \overline{w'\phi'} - \Delta F_\phi. \quad (20)$$

In the absence of a mass flux out of the ABL, i.e.,  $\overline{w'\phi'}_+ = 0$ ,

$$h \frac{D\hat{\phi}}{Dt} = \mathcal{D}h \Delta_+\phi + \overline{w'\phi'}_0 - \Delta F_\phi. \quad (21)$$

At first glance (21) appears not to involve mixing between the free troposphere and the ABL. However, this mixing is implicit in the first term on the RHS, as for fixed  $h$  the mass budget implies  $E = \mathcal{D}h$  when  $M = 0$ . In this limit, the mixing between the ABL and free troposphere is one way, i.e., the boundary layer is incapable of modifying the free-tropospheric state. The  $M = 0$  limit is problematic for  $\mathcal{D} < 0$ , as in this case there is no process whereby a steady-state ABL depth can be expected. However, in such cases one would expect a mass flux out of the ABL; choosing this mass flux consistent with the assumption of fixed ABL depth requires:

$$h \frac{D\hat{\phi}}{Dt} = -(\mathcal{D}h + M) \Delta_+\phi + \overline{w'\phi'}_0 - \Delta F_\phi. \quad (22)$$

In the non-entraining limit, with  $\mathcal{D} > 0$ ,  $M = -\mathcal{D}h$  and the first term on the RHS of (22) vanishes.

Equation (22) is identical in form to what one gets by considering the budget of  $\bar{\phi}$  over a layer of fixed depth in the case when  $\overline{w'\phi'}$  is modeled by a diffusivity,  $K$ , i.e.,

$$\overline{w'\phi'} = -K \partial_z \bar{\phi}, \quad \text{with } K = \ell M \quad (23)$$

where  $\ell$  is a length-scale implicit in the definition of the derivative. To maintain consistency with the implied ABL mass balance, the adjustment of the free-troposphere temperature profile through a mass-flux out of the ABL (for instance through a cumulus adjustment scheme) should, in the limit of a steady-state ABL depth, be balanced by commensurate amounts of entrainment mixing, e.g., per Eq. (22). In other words, models that employ flux-gradient relations of the form (23), yet wish to rationalize their exchange rules based on our current understanding of boundary layer processes, should incorporate the mass flux  $M$  in their specification of  $K$ . Moreover, given some  $K$  it becomes redundant to additionally specify  $E$ .

### 3.3 Energetics

A starting point for a consideration of the bulk energetics is the equation for the turbulence kinetic energy defined here as:

$$e \equiv \frac{1}{2} \left( \overline{u'^2} + \overline{v'^2} + \overline{w'^2} \right). \quad (24)$$

From the governing equations for the velocity field it is straightforward to show that for the case when departures from mean-flow homogeneity do not contribute to the shear production of turbulence (i.e., terms involving  $\nabla \bar{\mathbf{u}}$  and  $\partial_z \bar{w}$ ,  $\nabla \bar{w}$ )

$$\partial_t \bar{e} + \bar{\mathbf{u}} \cdot \nabla \bar{e} + \bar{w} \partial_z \bar{e} = -\overline{\mathbf{u}'w'} \cdot \partial_z \bar{\mathbf{u}} + \mathcal{B} - \partial_z \left[ \frac{1}{\rho_0} \overline{w'p'} + \overline{w'e'^2} - \nu \partial_z \bar{e} \right] - \varepsilon, \quad (25)$$

where  $e' = (1/2)(u'^2 + v'^2 + w'^2)$ ,  $\varepsilon$  is the molecular dissipation and  $\mathcal{B} \equiv \overline{w'b'} = g\overline{w'\theta'_v}/\theta_{00}$  defines the buoyancy flux. The first term on the RHS represents the conversion of mean-flow kinetic energy into turbulence kinetic energy,  $\mathcal{B}$  measures the buoyant production of  $\bar{e}$  at the expense of potential energy, or (if negative) the consumption of  $\bar{e}$  in favor of potential energy. The remaining three-component term describes various conservative forces which, barring contributions at the boundaries of the flow, simply serve to redistribute turbulence kinetic energy.

Insight into the energetics of simple buoyancy driven layers can be obtained by integrating (25) over the depth of the boundary layer [following (11)] and assuming that the fluxes of  $e$  vanish at the surface and  $h_+$ , and that the bounding surface does not do work on the ABL, in this case

$$\frac{D}{Dt} \hat{e} = \hat{\mathcal{B}} - \hat{\varepsilon} - \frac{E}{h} \hat{e}, \quad (26)$$

where  $E$  is given by (13) with  $M = 0$ . For the case when  $h$  is the only length-scale, one can posit the existence of a velocity scale,  $w_*$ , which nondimensionalizes the dissipation, such that  $\varepsilon h/w_*^3$  is universal. In equilibrium (26) implies that in the limit  $E/w_* \ll 1$ ,

$$w_*^3 \propto h \hat{\mathcal{B}}. \quad (27)$$

Such a scaling can also be justified using arguments from the theory of homogeneous isotropic turbulence, in which case  $w_*$  simply measures the strength of eddies of the scale  $h$  assuming that the turbulence in the boundary layer scales following Kolmogorov's inertial subrange scaling for dissipation rates equal to  $\hat{\varepsilon}$ . Evaluation of  $\hat{\mathcal{B}}$  requires a determination of the profile of  $\mathcal{B}$ . From the definition of  $\theta_v$ , it can be linearly related to fluxes of state variables, i.e.,

$$\mathcal{B} = \partial_s b|_{p,q} \overline{w's'} + \partial_q b|_{p,s} \overline{w'q'} \quad (28)$$

where the partial derivatives,  $\partial_s b$ ,  $\partial_q b$  take on very different values<sup>2</sup> depending on whether or not the layer is saturated [9, 10, 37]. Thus knowledge of the profile of  $\mathcal{B}$  depends on the profiles of  $\overline{w's'}$  and  $\overline{w'q'}$  and the state of the system (e.g., to determine whether the layer is saturated or not at a particular level). In the absence of sources, and in steady state the flux profiles are just constant. However, for many problems the assumption of stationarity is too strong, and a weaker constraint, called quasi-stationarity is employed. A quasi-steady layer is defined to be one satisfying

$$\partial_t (\partial_z \bar{\phi}) = 0. \quad (29)$$

Differentiating (10) by  $z$  (29), which says that the shape of the expected profiles is constant in time, is equivalent to requiring that  $\overline{w'\phi'} + \bar{F}_\phi$  is linear with  $z$ . Thus given  $\bar{F}_\phi$  and the boundary fluxes, the profile of  $\mathcal{B}$ , and hence the energetics of the layer, are straightforward to calculate.

Quasi-steadiness can be expected to hold as long as the boundary forcings are changing on timescales much longer than a turbulent timescale,  $t_* = h/w_*$ . Because  $w_*$  is typically near unity, for an ABL depth of  $h \approx 600$  m  $t_* \approx 10$  min and hence quasi-steadiness is often a useful constraint. Applying it to a convective

<sup>2</sup> Formally  $b$ , the buoyancy, is a function of the state  $(p, q, s)$  of the system, in which case the discontinuity of the partial derivatives  $\partial_q b$ ,  $\partial_s b$  is simply the definition of a first-order phase transition.



ABL for which it is typically assumed that  $\mathcal{B}_- = -\kappa\mathcal{B}_0$ , quasi-steadiness allows us to evaluate (27), from which it follows that by setting the constant of proportionality to  $2/(1 - \kappa)$

$$w_* = (\mathcal{B}_0 h_+)^{\frac{1}{3}} \quad (30)$$

which defines  $w_*$  as the velocity scale first introduced by Deardorff [11] to scale the dry convective boundary layer. For this reason (27) with a constant of proportionality of  $2/(1 - \kappa)$  is often used as a generalized convective velocity scale, which at times is questionable because the underlying assumption of  $h$  being the only independent length-scale is not generally justified. For instance in stratocumulus for which  $\mathcal{B}$  is discontinuous across  $z = \eta$ , the cloud-base height appears naturally as an additional length-scale [41].

### 3.4 Well-mixed limit

Bulk models are often equated with mixed-layer theory, in which it is assumed that the bulk layer is effectively homogenized by turbulence. This is because many of the assumptions which allowed us to derive (14)–(16) follow straightforwardly from the assumption that profiles of thermodynamic quantities are well mixed, i.e.,  $\overline{\phi} = \hat{\phi}$  for  $z \leq h$ . The well-mixed assumption also justifies the use of surface-layer similarity theory to specify the surface exchange coefficient  $C$  in terms of known quantities, and clarifies the relationship between  $M$  and  $E$ . An assumption about the vertical profile of the state variables also allows one to diagnose where clouds are to be expected, as well as their properties, which is necessary to compute radiative profiles, and hence  $\overline{F}_s$ , as well as the energetics of the layer. Although the assumption of well-mixedness does not change the form of (14)–(16), it does make it easier to rationalize the closure assumptions necessary to determine  $\overline{F}_s$ ,  $V$ ,  $M$  and  $E$  and hence the application of the bulk theory. However, as shall become apparent, these advantages of mixed layers have more to do with the fact that the theory makes an explicit statement about the structure of the thermodynamic profiles within the layer, and less to do with the details of that particular statement.

## 4 Stratocumulus

In this section we review the use of bulk theory to explain the structure and dynamics of the stratocumulus-topped ABL. Because the turbulence in stratocumulus-topped boundary layers is so often effective in maintaining a well-mixed state, we restrict ourselves to this limit. We begin in Sect. 4.1 by taking advantage of a very simplified representation of the entrainment velocity,  $E$  to construct a minimal representation of the stratocumulus-topped mixed layer. So doing allows us to explore analytically how the equilibrium structure depends on various parameters (Sect. 4.2), as well as the ways in which the layer adjusts to equilibrium (Sect. 4.3). The emergence of multiple equilibria is discussed briefly in Sect. 4.4, and the effects of more realistic representations of entrainment are discussed in Sect. 4.5. In the latter section we explore the ability of the more realistic models to explain the observed climatology of stratocumulus.

### 4.1 Minimal model

Our minimal representation of stratocumulus, assumes that the flow is horizontally homogeneous (except at the level of the divergence, i.e.,  $\mathcal{D}$  is not assumed to vanish), the mass flux,  $M$ , vanishes, and the cloud is non-precipitating, so  $\overline{F}_q$  vanishes. This allows the radiative driving to be specified unambiguously by the symbol  $\overline{F}$ . Although  $\Delta F$  is related to the structure of the ABL, for our immediate purposes we can consider it constant. For sufficiently thick clouds (more than 100m deep) at night this is actually not a particularly limiting assumption.

With these assumptions the mixed-layer equations can be written as a system of three ordinary differential equations (ODEs):

$$\frac{dh}{dt} = E - \mathcal{D}h, \quad (31)$$

$$\frac{d\hat{s}}{dt} = \frac{E\Delta_+s - V\Delta_0s - \Delta F}{h}, \quad \text{and} \quad (32)$$

$$\frac{d\hat{q}}{dt} = \frac{E\Delta_+q - V\Delta_0q}{h}. \quad (33)$$

A specification of the large-scale state can be interpreted to mean a specification of  $V$ ,  $\mathcal{D}$  and the boundary values  $s_+$ ,  $q_+$ ,  $s_0$ , and  $q_0$ , in which case all that remains to close the system is a specification of  $E$ . For now we consider a simple, physically plausible, relation which simplifies the analysis, namely the case when the nondimensional entrainment,

$$\alpha \equiv \frac{E \Delta_+ s}{\Delta F} \quad (34)$$

is a constant of order unity. Heuristically this way of scaling  $E$  suggests that diabatic mixing is proportional to the rate of driving of the flow (as measured by  $\Delta F$ ) and inversely proportional to the stability of the interface at cloud top, as measured by  $\Delta_+ s$ . Closures that more faithfully respect the energetics of the system are evaluated in [42,46] as well as in Sect. 4.5.

## 4.2 Equilibria

With this model of  $E$  we can solve for steady states of the system (which we denote by subscript ‘ $\infty$ ’) as follows:

$$h_\infty = h_* \left( \frac{\alpha \sigma}{1 + \sigma - \alpha} \right), \quad (35)$$

$$s_\infty = s_0 - \Delta s \left( \frac{1 - \alpha}{\sigma} \right), \quad \text{and} \quad (36)$$

$$q_\infty = q_0 + \Delta q \left( \frac{\alpha}{1 + \sigma} \right), \quad (37)$$

where

$$h_* = \frac{\Delta F}{\mathcal{D} \Delta s} \quad \text{and} \quad \sigma = \frac{V \Delta s}{\Delta F}. \quad (38)$$

The height scale  $h_*$  measures the height the equilibrium boundary layer would obtain for  $\alpha = 1$ , wherein  $h$  becomes independent of  $\sigma$ . In the stratocumulus regions of the northeast Pacific typical parameter values are  $\mathcal{D} \approx 4 \times 10^{-6} \text{ s}^{-1}$ ,  $V \approx 0.008 \text{ m s}^{-1}$ ,  $\Delta s \approx 12.5 \text{ kJ kg}^{-1}$ , and  $\Delta F \approx 40 \text{ W m}^{-2}$  averaged over a diurnal cycle, yielding values of  $h_\infty \approx 800 \text{ m}$  and  $\sigma \approx 2.5$  [44]. In this respect it is worth noting that cloudy solutions driven with diurnally varying radiative forcing and averaged over the diurnal cycle do not differ appreciably from equilibrium solutions driven by diurnally averaged radiative forcings [50].

An interesting aspect of the equilibrium equations is that for reasonable parameter values they predict realistic equilibrium ABL depths. They also show that for increasing lower tropospheric stability, as measured by increasing  $\sigma$ ,  $q_\infty \rightarrow q_0$ . Because  $s_\infty < s_0$  for  $\alpha < 1$ , one expects moister ABLs, and hence lower cloud bases with increasing lower-tropospheric stability, which is consistent with the climatological data [16].

One can help fix these ideas by looking at the height of cloud base  $\eta$ . We can solve for  $\eta_\infty$  by recognizing that  $\eta$  is just the height  $z$  where  $q_s(T(s, z))$  (the saturation vapor specific humidity) is equal to  $q$ . Similarly,  $\eta_\infty$  is just the height  $z$  where  $q_s(T(s_\infty, z)) = q_\infty$ . To solve for  $z$  we need a tractable form for  $q_s$  and an expression for  $T$  in terms of  $s$  and  $z$ . The latter follows directly from the definition of  $s$  recognizing that  $q_1 = 0$  at cloud base; the former we obtain by linearizing the logarithm of the dependence of saturation vapor pressure about the surface temperature such that

$$q_s(T) = q_s(T_0) \exp \left[ \frac{L}{R_v T_0^2} (T - T_0) \right]. \quad (39)$$

Noting that because the lower surface is saturated, i.e.,  $q_s(T_0) = q_0$ ,

$$q_\infty = q_0 \exp \left( -\frac{\Delta F}{g \eta_* V} (1 - \alpha) \right) \exp \left( \frac{-\eta_\infty}{\eta_*} \right) \quad \text{where} \quad \eta_* = \frac{R_v s_0^2}{L c_p g} \approx 1500 \text{ m}. \quad (40)$$

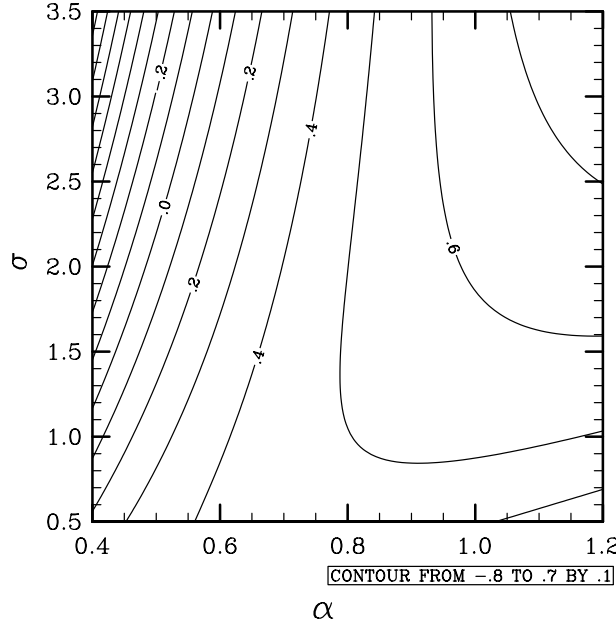


**Fig. 2** Equilibrium cloud-base height normalized by ABL depth as a function of  $\alpha$  and  $\sigma$

it is straightforward to arrive at the following explicit equation for  $\eta_\infty$ :

$$\eta_\infty = -\eta_* \ln \left( 1 + \frac{\alpha}{1+\sigma} \frac{\Delta q}{q_0} \right) - \frac{\Delta F}{Vg} (1 - \alpha). \quad (41)$$

Physically, the last term on the right arises because the temperature just above the surface is colder than the surface when  $\alpha < 1$ . This leads to lifting condensation levels being a few hundred meters lower than one would expect were they to assume that  $s_\infty = s_0$ . In the sub-tropics,  $q_+$  is very small compared to  $q_0$ , so that  $\Delta q/q_0 \approx -1$ . With this approximation, in the large- $\sigma$  limit,

$$\eta_\infty \rightarrow \eta_* \frac{\alpha}{1+\sigma} - \frac{\Delta F}{Vg} (1 - \alpha), \quad (42)$$

from which it is readily apparent that both larger  $\sigma$  and smaller  $\alpha$  favor the lowering of cloud base.

Of course one should hesitate to associate small  $\eta$  with a high probability of cloud incidence. A better measure would be the ratio  $\eta/h$ . From (35) and (41) in equilibrium this ratio is,

$$\frac{\eta_\infty}{h_\infty} = -\frac{\eta_*}{h_*} \left[ \frac{\ln \left( 1 + \frac{\alpha}{1+\sigma} \frac{\Delta q}{q_0} \right)}{\sigma \alpha} (1 + \sigma - \alpha) \right] - \frac{\Delta F}{Vgh_*} \left[ \frac{(1 - \alpha)(1 + \sigma - \alpha)}{\sigma \alpha} \right]. \quad (43)$$

Equation (43) is plotted in Fig. 2. Cloudy equilibria are expected when  $\eta_\infty/h_\infty < 1$ . The figure shows that this ratio decreases markedly with decreasing  $\alpha$ , and is relatively insensitive to  $\sigma$ . This tells us that, as entrainment becomes less efficient, the nondimensional thickness of the cloud layer increases. This makes physical sense. The free troposphere tends to be both warmer and drier than the ABL, thus enhanced entrainment can be expected to increase the lifting condensation level more rapidly than  $h$ . The marked sensitivity of the solutions to  $\alpha$  motivates a tremendous amount of research in this area [18,21–23,26,27,42].

### 4.3 Adjustment

The governing system of equations are weakly nonlinear due to the inverse dependence on  $h$  in (32) and (33) and from the dependence of  $\Delta_+ s$  on  $\hat{s}$  in the model of  $E$ . Linearizing (31)–(33) about its equilibrium state

effectively amounts to fixing  $E = E_\infty$  in (31) and (33) and setting  $h = h_\infty$  in the denominator of Eqs. (32) and (33). Analysis of this linearized system yields three real eigenvalues,

$$\lambda_1 = -\mathcal{D}, \quad \lambda_2 = -\mathcal{D} \left( \frac{1 + \sigma - \alpha}{\alpha} \right), \quad \text{and} \quad \lambda_3 = -\mathcal{D} \left( \frac{(\sigma + \alpha)(1 + \sigma - \alpha)}{\alpha \sigma} \right) \quad (44)$$

which are all negative if  $\mathcal{D} > 0$  and  $\alpha < 1 + \sigma$ , thus defining the domain of stable solutions. In the more general case, when  $\alpha = \alpha(h)$ , stability demands that  $\partial_h \alpha < \mathcal{D}$ . Such an analysis could be similarly extended to the more realistic case, when  $\alpha = \alpha(s, q, h)$ .

Roughly speaking the inverse of these eigenvalues corresponds to the timescale on which perturbations in  $h$ ,  $s$  and  $q$  are damped, which for typical parameter values evaluates to roughly 70, 30 and 20 h, respectively. On such timescales, one expects the advective terms in the substantial derivatives, e.g.,  $\hat{\mathbf{u}} \cdot \nabla \phi$ , to be significant [37,38], which motivates their inclusion in our subsequent analysis below. We also note that the clear separation between these timescales and those associated with the turbulence itself (tens of minutes) justifies the quasi-steady assumptions often used to constrain the energetics.

#### 4.4 Multiple equilibria

The system we have considered has only a single equilibrium. However, when one allows for the radiative forcing,  $\Delta F$ , to depend on the cloudiness, and for other processes (such as turbulence generated by shear at the surface) to engender entrainment it is possible to have multiple equilibria and hysteresis. An example of this behavior was shown by [33] using a simple model of shear-generated turbulence. The multiple equilibria for their model consisted of a shallow cloud-free ABL, and a deeper cloudy ABL.

#### 4.5 Realistic entrainment formulations

To evaluate the utility of equilibrium solutions of the mixed layer theory qualitatively, in Fig. 3 we show solutions computed using the June, July and August 1983–2001 climatology as extracted from the 40+ year reanalysis of meteorological data by the European Center for Medium-Range Weather Forecasts [48, e.g., the ERA40]. The climatology was used to specify the surface and free tropospheric state, with the divergence of the near-surface winds being substituted for  $\mathcal{D}$ . In computing these solutions, the radiative forcing was fixed at  $40 \text{ W m}^{-2}$  and advective tendencies were added based on gradients characteristic of the mean stratocumulus regions of the northeast Pacific ( $\nabla q = 1.2 \times 10^{-9} \text{ m}^{-1}$ ,  $\nabla s = 3.9 \times 10^{-3} \text{ m s}^{-2}$  and  $\nabla h = 1.4 \times 10^{-4}$ ), as derived from the ERA40, using their representation of ABL depth.

These solutions were computed using a state-of-the-art entrainment parameterization, for which the entrainment rate is determined by requiring the net buoyancy flux to be some fixed fraction of its value in the absence of entrainment [18]. Mathematically the closure amounts to finding which value of  $E$  results in a predetermined value of the ratio:

$$\alpha_B \equiv \hat{\mathcal{B}} / \hat{\mathcal{B}}_{E=0}, \quad (45)$$

where  $\hat{\mathcal{B}}_{E=0}$  denotes the average buoyancy flux in the absence of entrainment. Although straightforward, the evaluation of  $\hat{\mathcal{B}}$  and  $\hat{\mathcal{B}}_{E=0}$  is not trivial. Because the entrainment rate sets the thermodynamic fluxes at cloud top, which in turn are related to  $\mathcal{B}$  given the assumption of quasi-steadiness and the piecewise continuous relations in (28), fixing the ratio per (45) is sufficient to determine  $E$ . This fixed- $\alpha_B$  closure is similar in spirit to the fixed- $\alpha$  closure discussed earlier, but by integrating the actual and zero entrainment buoyancy fluxes, it more accurately accounts for the energetics. It is chosen because it is conceptually simple, yet has fared well (with  $\alpha_B \approx 0.2$ ) in past evaluations based on both large-eddy simulation and field data [46].

The solutions in Fig. 3 plausibly represent the well-known regions of stratocumulus convection, over the eastern boundary currents of the subtropical oceans. In qualitative agreement with climatology four main regions appear [16]. In the NE Pacific near  $120^\circ\text{W}$  and  $30^\circ\text{N}$ ; in the SE Pacific near  $80^\circ\text{W}$  and  $20^\circ\text{S}$ ; in the N. Atlantic near  $20^\circ\text{W}$  and  $30^\circ\text{N}$ , and in the S. Atlantic near  $10^\circ\text{E}$  and  $20^\circ\text{S}$ . Over each of these regions the equilibria are characterized by shallow ABLs between 400 and 1,000 m topped by relatively thin stratocumulus layers, with liquid-water paths ( $\mathcal{L} \equiv \int_0^h \rho_0 q_l dz$ ) generally less than  $400 \text{ g m}^{-2}$ . Because deviations in the well-mixed assumption, which are small from the perspective of the budgets of  $q$  and  $s$ , can have a large

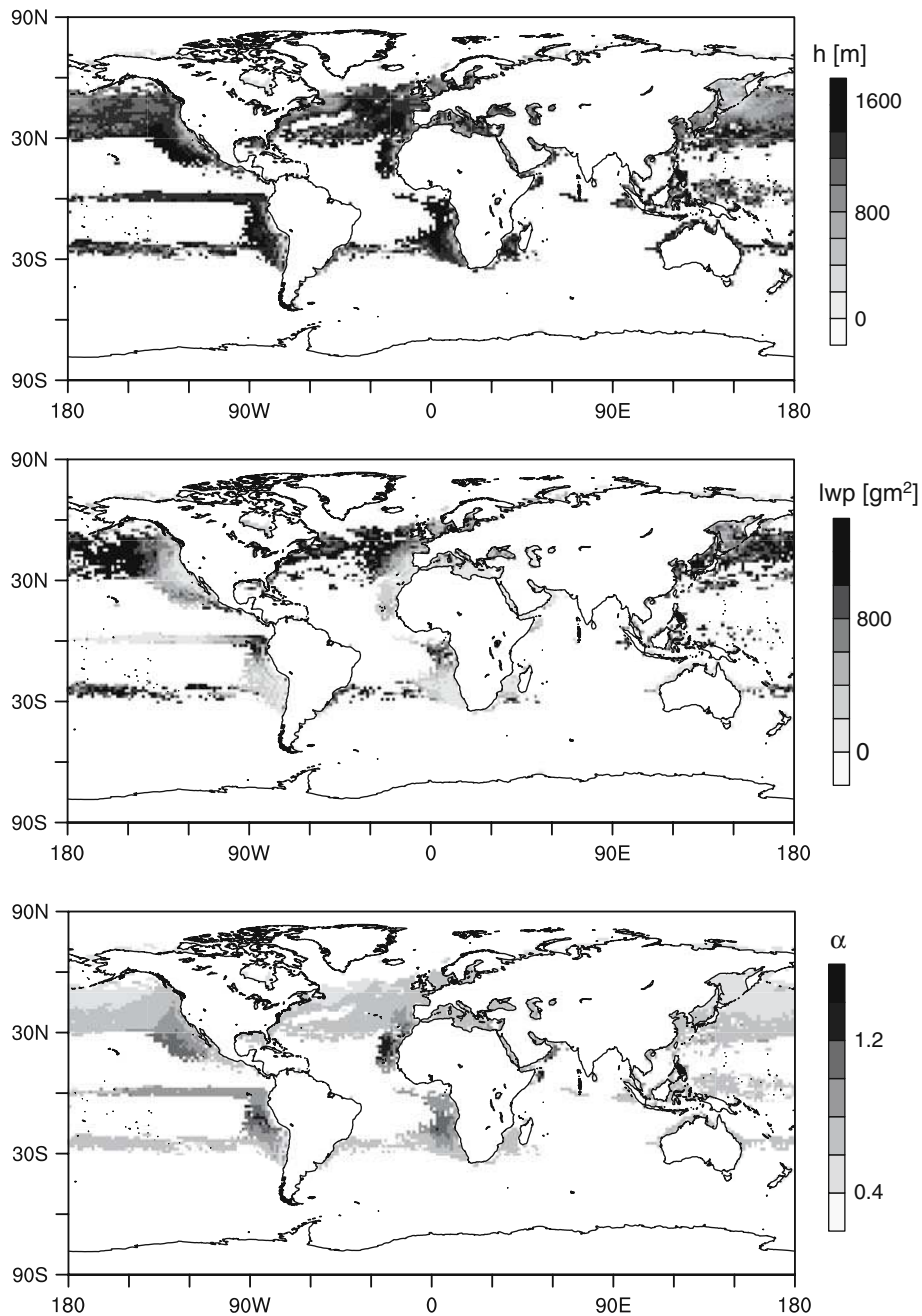


**Fig. 3** Equilibrium solutions using ERA40 climatological forcing for June, July and August, with  $\alpha_B = 0.25$ , constant advective forcings and fixed radiative cooling representative of mean stratocumulus regions. From top to bottom,  $h$ , liquid water path  $\mathcal{L}$ , and  $\alpha$ . Values with  $\mathcal{L} > 1,400 \text{ g m}^{-2}$ , or  $h > 2,000$  are masked

impact on the equilibrium value of  $q_1$ , we relax the well-mixed assumption when calculating the liquid-water path to two thirds of its adiabatic value, making it more commensurate with commonly observed values [44].

The model also produces equilibria over the storm tracks in the northern hemisphere and along thin bands over the equatorial cold tongue of the Pacific and over both the Pacific and Atlantic oceans near  $25^\circ\text{S}$ . Although these also tend to be regions of significant low cloudiness, the equilibrium solutions in these areas tend to have such thick clouds that precipitation and other processes will become important. This suggests that the stratocumulus regions may be well captured by the model after being masked for equilibria whose cloud depths are incompatible with the assumption of no, or little, precipitation.

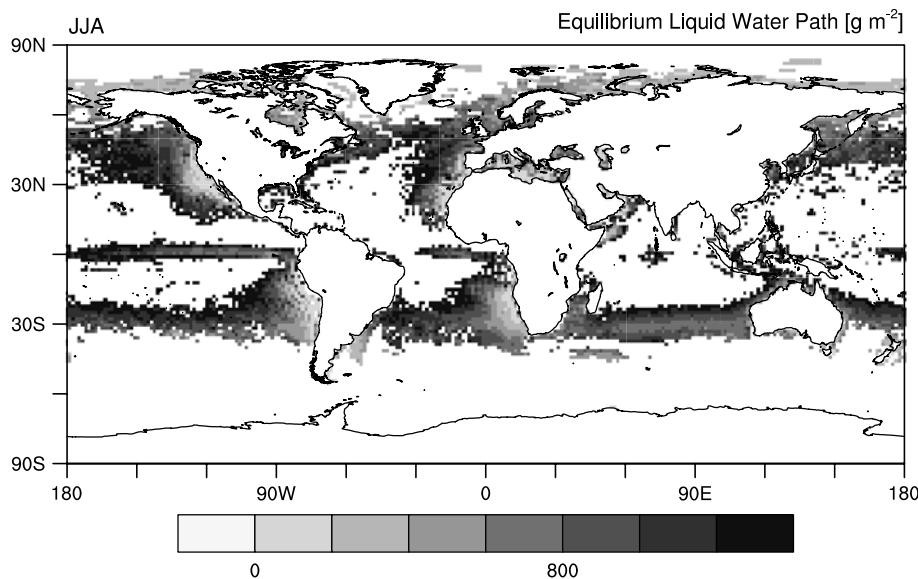


**Fig. 4** Equilibrium solutions for  $\alpha = 0.85$  and boundary and forcings as in Fig. 3

Another basis for flagging solutions of the model is by measuring the value of  $\alpha = E\Delta_+s/\Delta F$  that the fixed  $\alpha_B$  parameterization produces in equilibria. Values of  $\alpha > 1$  are indicative of other processes (surface and latent heat fluxes) contributing significantly to the energetics of the layer. In a remarkably insightful study Bretherton and Wyant [9] show that in this limit the amount of entrainment warming can be larger than the radiative cooling of cloud-top air parcels, and thus while evaporation of liquid water may fuel parcel descent through the cloud layer, their positive buoyancy in the sub-cloud layer will resist further descent, thus encouraging the thermodynamic differentiation between the cloud and sub-cloud layer and more cumulus-like cloud circulations. Formally this transition can be associated with buoyancy fluxes just below cloud base, reaching the limit associated with the dry convective ABL, i.e.,  $\mathcal{B}_\eta = -\kappa\mathcal{B}_0$ , [41], which in practice often amounts to  $\alpha > 1.1$  or so [47]. So although Fig. 3 is masked based on values of  $h > 2,000$ , these regions are invariably associated with  $\alpha > 1.1$  and thus could be just as effectively masked by this energetic constraint.

In either case, the transition of the equilibria to higher values of  $\alpha$  as the flow advects westward and equatorward away from the eastern boundary currents of the subtropical oceans is indicative of a greater propensity toward lower cloud fractions and more cumulus-like circulations, consistent with observations of this evolution. More quantitative evaluations will be presented elsewhere, and although not shown, the seasonal cycle is also qualitatively captured by this approach, with cloudiness in the southern oceans peaking in September–October–November as observed. Moreover, the inclusion of more realistic (spatially varying) advective effects leads to further improvement in the solutions.

For the sake of applying these types of approaches to modeling the stratocumulus topped ABL in very simple models of larger-scale circulations we note that  $\alpha$  does not vary tremendously over the solution region in Fig. 3, which suggests that the much simpler fixed- $\alpha$  model may have utility. In Fig. 4 we show the climatology of equilibrium solutions with  $\alpha = 0.85$  here again the area of modest liquid-water paths ( $< 500 \text{ g m}^{-2}$ ) well inscribe the stratocumulus regions. Because such a model permits algebraic solutions, but is formally related to much more sophisticated representations of stratocumulus, its equilibrium solutions may provide a useful alternative to purely empirical parameterizations of stratocumulus currently used in many models of simplified tropical dynamics.

## 5 Trade-wind cumulus

In contrast to stratocumulus, the trade-wind layer is less obviously a single layer: past work has emphasized distinctions between the cloud and sub-cloud layer, as well as the mediating influence of thin layers near cloud base (the transition layer) at the surface, and at the top of the cloud layer (e.g., Fig. 1 in [29]). As a result a variety of bulk models have been developed to represent such effects, a subset of which are discussed in turn

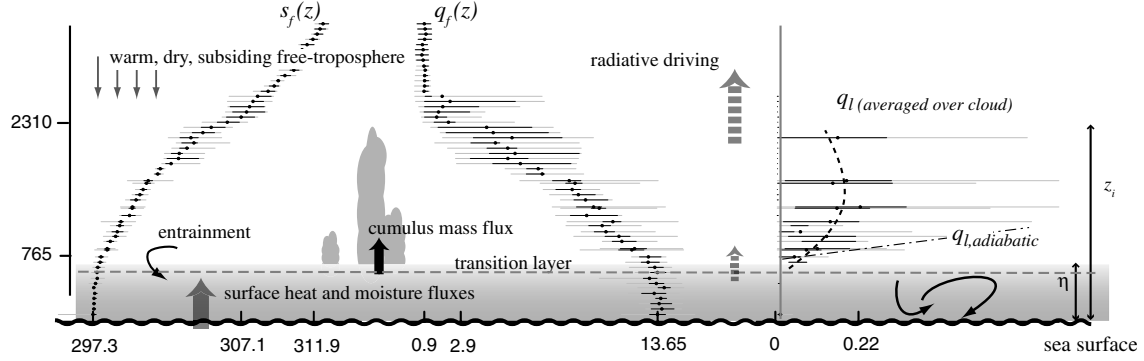


**Fig. 5** Structure of the cumulus-topped boundary layer as observed during the tenth research flight of the *Rain in Cumulus over the Ocean Field Study*. The ordinate shows the top of the cloud layer and the LCL of the mean surface layer air. The values on the  $x$ -axis give  $s/c_p$  averaged over the sub-cloud layer, at 2,300 and at 3,500 m for the left panel;  $q$  at 3,500, 2,300 m and averaged over the sub-cloud layer for the middle panel; and the liquid-water specific humidity over cloud passes only (where cloud coverage is typically 5–10%) in the rightmost panel. Basic processes determining the thermodynamic structure of the cloud and sub-cloud layers are indicated schematically. Plotting conventions otherwise as in Fig. 1

below. First in Sect. 5.1 we explore a bulk description that encompasses the cloud layer, and then in Sect. 5.2 we explore a bulk representation of only the sub-cloud layer. Because the same notation takes on different meanings in the different situations (for instance the layer just above the bulk layer refers to the free troposphere in the former case and the cloud layer in the latter) care should be taken when comparing expressions between the two sections.

### 5.1 One-layer models

A well-known bulk model of the trade-wind regime is that developed by Betts and Ridgway [7]. The model incorporates the entirety of the trade-wind layer, from the surface to cloud-top, into a single layer. Choosing  $h$  to represent the entirety of the layer (i.e., associating it with  $z_i$  in Fig. 5) avoids the problem of dealing with a model of the mass flux and so, as with stratocumulus, the system can be represented by (14)–(16) with  $M = 0$ .

By considering only non-advective steady-state solutions Betts and Ridgway substitute for  $E$  in (15) and (16) with  $\mathcal{D}h$  as implied by the steady-state mass balance. In this case the heat (enthalpy) and moisture budgets become

$$0 = \mathcal{D}h \Delta_+ s + \overline{w' s'_0} - \Delta F \quad (46)$$

$$0 = \mathcal{D}h \Delta_+ q + \overline{w' q'_0}. \quad (47)$$

The model amounts to an exploration of the above constraints under the assumption that: (1) the vertical structure of the state variables within the ABL is well described by a prescribed form (a mixing line [6]); and (2) that the surface flux  $\overline{w' \phi'_0}$  (for  $\phi \in \{s, q\}$ ) is well modeled by (13) with  $V$  determined by surface-layer similarity and  $\hat{\phi}$  replaced by  $\phi_m$  in  $\Delta_0 \phi$ , where the subscript  $m$  denotes a value in the sub-cloud mixed layer.

To illustrate the behavior of their model we specify an analogous vertical structure as follows:

$$\bar{\phi} = \begin{cases} \phi_m & z < \eta \\ \phi_m + \left(\frac{z-\eta}{h-\eta}\right) (\phi_- - \phi_m) & z \geq \eta \end{cases} \quad \text{where } \phi_- = (1 - \beta_-) \phi_m + \beta_- \phi_+; \quad (48)$$

and recall that  $\eta$  denotes the height of the lifting condensation level and thus measures the depth of the sub-cloud layer, while  $\phi_- \equiv \bar{\phi}_{z=h_-}$  measures the state-variable properties just below cloud top and follows from the assumption that the cloud layer lies on a mixing line defined by the parameter  $\beta_- < 1$ . Integrating (48) over the layer yields

$$\hat{\phi} = \phi_m + \zeta (\phi_+ - \phi_m) \quad \text{where } \zeta = \frac{\beta_-}{2} \left(1 - \frac{\eta}{h}\right), \quad (49)$$

where  $\zeta$  is a nondimensional height.<sup>3</sup> This definition of the vertical structure allows us to write the heat and moisture budgets, i.e., (46) and (47), as

$$0 = \mathcal{D}h(1 - \zeta)(s_+ - s_m) + V(s_0 - s_m) - \Delta F, \quad (50)$$

$$0 = \mathcal{D}h(1 - \zeta)(q_+ - q_m) + V(q_0 - q_m). \quad (51)$$

Because  $s_+$  is known only as a function of  $h$ , after specifying  $\mathcal{D}$ ,  $V$ ,  $q_+$ ,  $\zeta$  and the SST, (50) and (51) retain three unknowns. Thus an additional constraint is required to close the system. This is provided by requiring the heat (enthalpy) budget (46) also to be balanced over the sub-cloud layer with

$$\mathcal{D}\eta(\bar{s}_{z=\eta+\epsilon} - s_m) = -\kappa V(s_0 - s_m), \quad (52)$$

i.e., the heat flux at the top of the sub-cloud layer is some fraction  $-\kappa$  of its surface value. Specifying  $\kappa = 0.25$  [7, in analogy to the well established behavior of the dry convective ABL] and demanding that the sub-cloud layer heat (enthalpy) budget is balanced determines  $s_m$  in terms of the radiative flux divergence across the sub-cloud layer, which we denote by  $\Delta_m F$ :

$$s_m = s_0 - \frac{\Delta_m F}{(1 + \kappa)V} \quad (53)$$

As was the case for stratocumulus, the model is closed by an entrainment assumption (e.g., 52); but in this case the constraint is enforced at cloud base, rather than at  $h$ . In this context it is worth noting that (e.g., Fig. 5) the jumps are less well defined, particularly in mean profiles, which due to the undulation of the transition layer, smooths out the local jumps at cloud base.

Evaluating (50)–(53) allows us to write the heat and moisture budget constraints as

$$s_m = s_0 \left(1 - \frac{\gamma}{1 + \kappa}\right), \quad (54)$$

$$q_m = \frac{q_0 + Rq_+}{1 + R}, \quad \text{and} \quad (55)$$

$$s_+ = s_0 \left[1 - \frac{\gamma}{R} \left(\frac{1 + R}{1 + \kappa} + N\right)\right] \quad (56)$$

where ideally the nondimensional parameters

$$\gamma = \frac{\Delta_m F}{s_0 V}, \quad N = \frac{\Delta F}{\Delta_m F}, \quad R \equiv \frac{\mathcal{D}h}{V}(1 - \zeta) \quad (57)$$

help highlight, rather than obscure, the structure of the model. With values typical for the trades, i.e.,  $\rho \Delta_m F = 12 \text{ W m}^{-2}$ ,  $\Delta F = 50 \text{ W m}^{-2}$ ,  $V = 0.01 \text{ m s}^{-1}$ , and  $\mathcal{D} = 3.5 \times 10^{-6} \text{ s}^{-1}$ , the above parameters are roughly 1/300, 5, and 0.5 respectively.

Because both  $R$  and the radiative fluxes (and hence  $N$  and  $\gamma$ ) depend on the structure of the ABL, (54)–(56) implicitly define the state of the system and must be solved iteratively. Equation (56) is actually an equation for the ABL depth, as  $h$  is determined by finding the height at which the specified free-atmospheric profile  $s_f$  matches  $s_+$ . Following the derivation leading to (41), given  $s_m$  and  $q_m$ , the lifting condensation level follows naturally as:

$$\eta_\infty = -\eta_* \ln \left[1 + \frac{\Delta q}{q_0} \left(\frac{R}{1 + R}\right)\right] - \frac{\gamma}{1 + \kappa} \left(\frac{s_0}{g}\right). \quad (58)$$

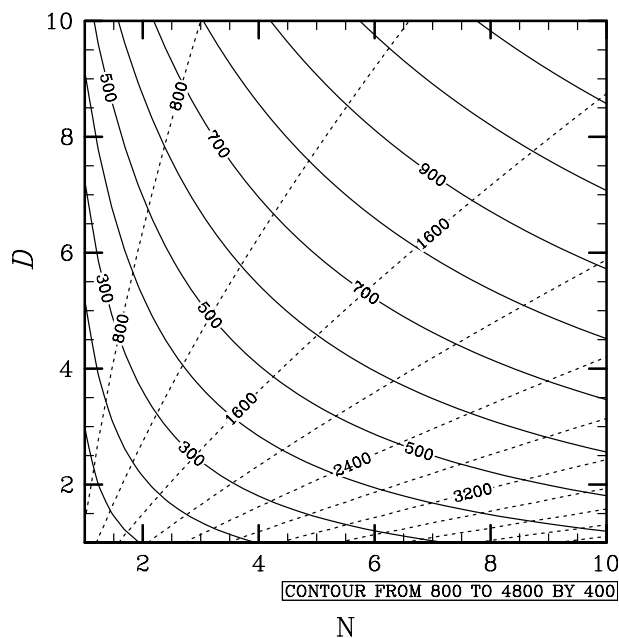
Betts and Ridgway solve the above system by using an elaboration of the assumed ABL structure (to account for differences between cloudy and non-cloud regions, presumed to exist in fixed proportions) in conjunction with a radiative transfer model to determine  $F$  and by specifying the product  $\mathcal{D}h(1 - \zeta)$  which appears in the definition of  $R$ . Doing so obscures the dependence of the solutions on  $\mathcal{D}$  and can yield solutions that are inconsistent with the assumed structure of the model, which in our case is determined by  $\beta_-$  and (48). We illustrate the behavior of the model in Fig. 6 by instead specifying the radiative fluxes and  $\mathcal{D}$ , with a consistent

<sup>3</sup> Betts and Ridgway denote this nondimensional height by  $\alpha$ , we use  $\zeta$  because  $\alpha$  is reserved for the stratocumulus entrainment efficiency.



**Table 3** Parameter values for use in the construction of Fig. 6

Parameter	Value
$\Delta_m F$	$12 \text{ W m}^{-2}$
SST	300 K
$q_+$	$3 \text{ g kg}^{-1}$
$V$	$0.01 \text{ m s}^{-1}$
$p_0$	1,013 hPa
$\kappa$	0.25
$\beta_-$	0.3

**Fig. 6**  $\eta_\infty$  and  $h_\infty$  (dashed) as a function of  $N$  and  $D \times 10^6$  for the parameter values in Table 3

value of  $R$  determined by iteration. So doing can generate an inconsistency between the assumed structure and the specified changes in the radiative fluxes across the layer, but more clearly illustrates the behavior the model for an externally specified forcing. In calculating these solutions we specify the free atmospheric profile of  $s$  so that  $s_+/c_p = 291.4 + 0.0058h$  K which is based on the mean structure of the atmosphere in the summertime trades of the northeast Pacific. Our choices for the values of other parameters are listed in Table 3, suffice to say that they are typical and taken from Betts and Ridgway [7]. With the help of Fig. 6, we note that with  $N = 5$  and  $D = 3.5 \times 10^{-6} \text{ s}^{-1}$ ,  $\eta \approx 600$  m and  $h \approx 1750$ . Values of  $\eta$  between 400 and 800 m and  $h$  between 1200 and 3000 m are realistic. The tendency for  $h$  to be more variable than  $\eta$  reflects the fact that the former is more sensitive to the dynamical state of the atmosphere as represented by  $D$ . As an aside, our calculations also confirm that the solutions are relatively independent of  $\beta_-$  and  $\kappa$ . Choosing  $\kappa = 0$  results in little change in  $h$  but lowers cloud base by roughly 20%; doubling  $\beta_-$  also has little effect on  $h$ , but lowers the cloud base by about 10%. Because for a well-mixed sub-cloud layer the height of cloud base effectively measures the partitioning of the surface fluxes among the sensible and latent components (i.e., the Bowen ratio) the sensitivity of  $\eta$  to  $\beta_-$  and  $\kappa$  measures the extent to which the partitioning of the surface fluxes is controlled by these parameters.

The reasonable value of solutions, their robustness, and their ability to respond sensibly to macroscopic changes in the large-scale state are all attractive elements of this model, and motivates its use in a variety of thermodynamic models of tropical circulations [7, 25, among others]. The disadvantage of using this system of equations as a basis for the ABL treatment in simplified models of tropical dynamics is that  $h$  varies considerably – reaching through the depth of the troposphere as the convecting zones are approached ( $D$  decreases). Incorporating the cloud layer into the ABL has advantages from the perspective of continuity with the upstream

stratocumulus layers, but disadvantages from the perspective of matching to regions of deeper, precipitating convection. Moreover, as  $h$  increases, some of the assumptions of the underlying equations (for instance, neglect of baroclinic effects) also become increasingly suspect. These reasons motivate an exploration of bulk models of just the sub-cloud layer, a topic which we address in Sect. 5.2.

A quite different weakness of the (54)–(56) is that the structure of the cloud layer is imposed by an a priori constraint [in our case (48)] and the only remaining physics in the model is through the closure assumption (52). Allowing the cloud layer structure to respond to the macroscopic structure of the ABL (i.e.,  $\eta$  and  $h$ ) provides an opportunity for physical insights, and important new feedbacks between the radiative driving of the layer and its bulk structure. Such effects could conceivably be included by letting  $\beta_-$ , or more generally (48), respond more realistically to the bulk state. Another approach to this weakness has been the exploration of two-layer models, which explicitly model the interaction between the cloud and sub-cloud layer, and the cloud layer and the free troposphere. A well-known model in this class is that devised by Albrecht [2] but because of unsatisfactory parameter sensitivities [8] and inconsistencies in its closure [4] this model is less widely accepted as a bulk theory of the trade-wind layer.

Before proceeding to other models of the trade-wind layers, we briefly point out some connections between the Betts and Ridgway model of the trade-wind layer and the bulk model of stratocumulus presented in §4. From (50) and (53), we note that the equilibrium solutions of the Betts and Ridgway model correspond to an entrainment rate,

$$E = \mathcal{D}h = \frac{1}{(s_+ - \widehat{s})} \left( \Delta F - \frac{4}{5} \Delta_m F \right) \quad (59)$$

which implies an entrainment efficiency (e.g., Sect. 4) of

$$\alpha \equiv \frac{E \Delta_{+s}}{\Delta F} = \left( 1 - \frac{4}{5N} \right). \quad (60)$$

For typical trade-wind situations  $N \approx 5$  and hence  $\alpha \approx 0.85$ . In principle this provides a basis for matching equilibrium stratocumulus solutions such as that described in Sect. 4 to trade-wind solutions.

The definition of the entrainment efficiency (60) allows one to define a dynamic system of equations for the Betts–Ridgway model equivalent to (31)–(33) but replace  $E$  with  $E + \zeta V$  in (32) and (33) to account for the effect of the vertical structure on the surface fluxes. Note that for a well-mixed layer  $\zeta = 0$  and hence the model reverts to the stratocumulus limit.

## 5.2 Sub-cloud layer models

As an alternative to a model of a single-bulk layer for the entirety of the trade-wind layer, it can prove convenient to simply consider the ABL as being confined to the sub-cloud layer. That is, in Fig. 5 we associate  $h$  with  $\eta$  as opposed to  $z_i$ . Consequently  $\widehat{\phi}$  now refers to just the sub-cloud layer values, what we called  $\phi_m$  in the previous section. Choosing just to investigate the bulk structure of the sub-cloud layer leads to shallower and less-variable values of  $h$  over the tropical oceans, more-constrained vertical structure, less possibility for baroclinic influence, and greater continuity with periods, or regions, of deeper convection. From such a perspective the governing system of equations are simply (14)–(16). In the stratocumulus limit (e.g., Sect. 4)  $M = 0$  and  $\phi_+$  is given the free-tropospheric values, thereby requiring only one additional constraint to close the system. In the trade-wind regime  $M \neq 0$  and  $\phi_+$  corresponds to values just above cloud base, in the cloud layer, and thus is not-known a priori. Hence closure of this system of equations over the sub-cloud layer in the trades requires four additional constraints. Typically these are applied as models for  $s_+$ ,  $q_+$  (in effect assuming the structure of the cloud layer),  $M$  and  $E$ .

An early pioneer of this approach was again Betts [5], who closed the system by writing additional budget equations for the transition layer to specify  $(s_+, q_+)$ , specifying  $E$  following the heat flux closure in (52), and by defining the mass flux,  $M$ , implicitly by setting  $h = \eta$ . Neggers et al. [29] revisit this approach with the aim of developing parameterizations of shallow convective ABLs for use in simplified climate models. In their approach they dispense with the transition layer equations and simply fix the transition layer jumps to be proportional to the difference between the free tropospheric and sub-cloud values:

$$\Delta_+ \phi = \beta_{\phi_+} (\phi_f - \widehat{\phi}) \quad (61)$$

for  $\phi \in \{s, q\}$ , where subscript  $f$  refers to the free-tropospheric value, which is presumed known. As a reminder, in this section  $\widehat{\phi}$  refers to the value of  $\phi$  averaged only over the *sub-cloud* layer. The entrainment flux is once again specified following the well-known dry convective limit, such that

$$E = -\kappa \mathcal{B}_0 / \Delta_+ b, \quad (62)$$

with

$$\Delta_+ b \equiv b_+ - \widehat{b} = \frac{g}{s_0} [\Delta_+ s + 0.608 s_0 \Delta_+ q] \quad \text{and} \quad \mathcal{B}_0 = -\frac{gV}{s_0} [\Delta_0 s + 0.608 s_0 \Delta_0 q] \quad (63)$$

denoting the buoyancy jump at  $h$  and the surface buoyancy flux respectively. Lastly the cloud-base mass flux is modeled as

$$M = \mathcal{A} w_* \quad (64)$$

where  $w_*$  is the Deardorff velocity scale give by (30) and  $\mathcal{A} > 0$  is the cloud fraction determined as a function of the state of the system. Except for (64) these closures are relatively standard. Equation (61) is effectively an assumption on the structure of the cloud layer. Equation (62), which can be equivalently phrased as an assumption that the entrainment buoyancy flux  $\mathcal{B}_-$ , is some fixed negative fraction  $\kappa$  of the surface buoyancy flux, is analogous to (52); its application to the buoyancy budget (rather than the heat budget) is standard for the dry convective layer and, notwithstanding arguments to the contrary [7], and more appropriate to cumulus topped ABLs as well [40,41,43]. As Neggers et al. [28,29] and Nicholls and LeMone [30] point out, the form of (64) dates back to much earlier studies, but relating  $\mathcal{A}$  to the cloud fraction is a relatively recent trend.

An interesting aspect of the above model is that it predicts regions of cloud-free solutions, effectively those regions where the steady-state  $h$  is less than  $\eta$  for  $M = 0$ . If advective and radiative processes are negligible compared to mixing processes in the cloud layer, then  $s_+$  and  $q_+$  can be expected to lie on a mixing line, in which case  $\beta_{s_+} = \beta_{q_+} = \beta_+$ , and the equilibria take the form

$$h_\infty = \frac{E}{D}, \quad (65)$$

$$\widehat{s}_\infty = \frac{Vs_0 + \beta_+ E s_f - \Delta F}{V + \beta_+ E}, \quad \text{and} \quad (66)$$

$$\widehat{q}_\infty = \frac{Vq_0 + \beta_+ E q_f - h\widehat{\mathbf{u}} \cdot \nabla q}{V + \beta_+ E}, \quad (67)$$

where

$$E = \frac{\kappa}{\beta_+} V \left( \frac{\Delta F + 0.608 s_0 h\widehat{\mathbf{u}} \cdot \nabla q}{\Delta F_s + 0.608 s_0 h\widehat{\mathbf{u}} \cdot \nabla q + (1 + \kappa)V(\Delta s + 0.608 s_0 \Delta q)} \right). \quad (68)$$

Following Neggers et al. the radiative forcing  $\Delta F$  and the advective tendency in the moisture equation ( $h\widehat{\mathbf{u}} \cdot \nabla q$ ) are retained so as to represent both advective and radiative effects. Neggers et al. found the advective contribution to the evolution of  $s$  to play less of a role, and neglected it, thus motivating its absence above. Given  $\widehat{s}$  and  $\widehat{q}$ , it is straightforward to show that

$$\eta_\infty = \frac{\Delta_0 s}{g - \eta_* \ln(\widehat{q}/q_0)}. \quad (69)$$

Cloud-free solutions thus correspond to solutions where  $\eta > h$ . For  $\eta < h$  we expect cloudy solutions. For these we note from (68) that for a fixed forcing,<sup>4</sup> and  $s_f$  constant with height,  $E$  is independent of  $h$ , which implies  $\widehat{s}$  and  $\widehat{q}$  and hence  $\eta$  are also independent of  $h$ . Consequently  $M$  can be solved for directly, simply by noting that in this situation  $h = E/D$  and that, in so far as the mass flux principally acts to ventilate the ABL, thereby relaxing  $h$  to  $\eta$ , choosing  $M = E - D\eta$  must be true in equilibrium; in this case the equilibrium cloud fraction is just

$$\mathcal{A} = \frac{E - D\eta_\infty}{w_*}. \quad (70)$$

<sup>4</sup> i.e.,  $s_f$ ,  $\Delta F_s$  and  $h\widehat{\mathbf{u}} \cdot \nabla q$  constant.

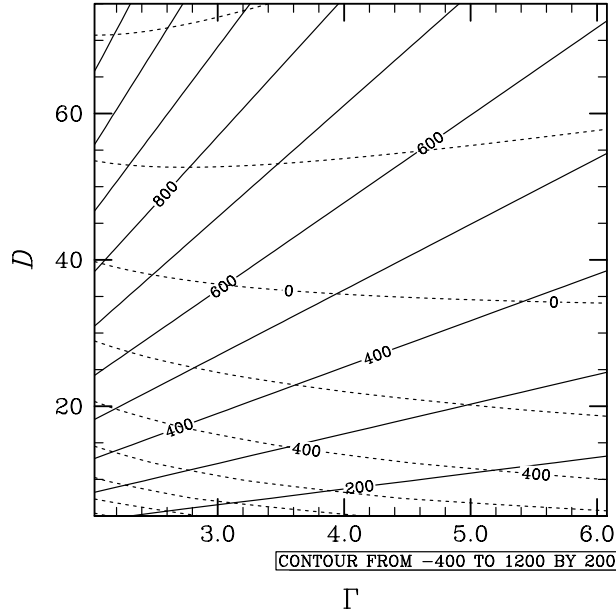


**Fig. 7** Equilibrium  $\eta$  (solid) and  $h - \eta$  (dashed) as a function of  $\mathcal{D} \times 10^{-6}$  and  $\Gamma$ , with other parameters as specified in Table 3, and  $\Delta F$  and  $h\hat{\mathbf{u}} \cdot \nabla q$  taken as 15 and  $30 \text{ W m}^{-2}$ , respectively, consistent with the values chosen by [29] for a 750-m-deep sub-cloud layer

For typical values of  $E \approx 1 \text{ cm s}^{-1}$ ,  $D = 3 \times 10^{-6} \text{ s}^{-1}$ ,  $\eta = 500 \text{ m}$  and  $w_* = 0.6 \text{ m s}^{-1}$ ,  $E \gg D\eta$ , and  $\mathcal{A} \approx E/w_* \approx 0.02$ , which might explain why the cloud fraction is of the order of a few percent.

This special (albeit somewhat contrived) limit of constant forcings and  $s_f$  independent of height highlights the role of  $\beta_+$ . Because  $E \propto \beta_+^{-1}$  but the heat and moisture budgets depend only on the product  $\beta_+ E$ , both  $\hat{s}$  and  $\hat{q}$ , and hence  $\eta$  must be independent of  $\beta_+$ . Thus, in this limit,  $\beta_+$  plays no role in determining the strength of the surface fluxes, or the height of the sub-cloud layer, but instead simply determines the depth of the equilibrium layer whose mass flux is zero – and by implication the mass flux for models of  $M$  that act to ventilate the ABL, thus relaxing  $h$  to  $\eta$ .

Perhaps a more realistic situation is obtained by letting  $s_f$  vary with height. In principal,  $s_f$ ,  $\Delta F$ , and  $h\hat{\mathbf{u}} \cdot \nabla q$  should all depend on the structure of the trade-wind layer, but here we only consider  $s_f$  varying with height as  $s_f/c_p = 301 + \Gamma h$ . Because  $s_f$  really is determined by the height of cloud top and  $h$  is intended to model the cloud base height, this is at best a modest improvement. These limitations notwithstanding, Fig. 7 shows the  $M = 0$  solutions of (65)–(67), for  $\beta_+ = 0.2$  and the aforementioned model of  $s_f$  as a function of  $\mathcal{D}$  and  $\Gamma$ . Because of the  $h$  dependence of  $s_f$  they are obtained iteratively. The solid lines show contours of  $\eta$  while the dashed lines show  $h - \eta$ . Thus cloud-free ( $M = 0$ ) solutions are associated with negative dashed contours and the zero contour marks the values of  $\mathcal{D}$  and  $\eta$  at which  $h = \eta$ . If we denote these values of  $\mathcal{D}$  by  $\mathcal{D}_*$  then for some  $\mathcal{D} < \mathcal{D}_*$  the equilibrium mass flux can be inferred as  $M = (\mathcal{D}_* - \mathcal{D})\eta$ . From Fig. 7 we note that  $\mathcal{D}_* \approx 3.5 \times 10^{-5}$  and  $\eta$  varies between values just below 400 m to just above 800 m. Because typical values of  $\mathcal{D}$  in the trades are an order of magnitude less than  $\mathcal{D}_*$  these results suggest that  $\eta$  increases with decreasing stability and that  $M \approx 2.5 \text{ cm s}^{-1}$ , consistent with the results of Neggers et al. [29]. These simple calculations indicate that the model does provide a useful description of the equilibrium state of the sub-cloud layer, and thus could prove beneficial in a variety of contexts as discussed in Sect. 1. A more thorough evaluation, which complements the analysis of the stratocumulus layer in Sect. 4.5 is provided by [29].

One unsatisfactory aspect of this class of models is their dependence on a seemingly poorly constrained parameter,  $\beta_+$ . For the solutions in Fig. 7, halving  $\beta_+$  effectively doubles  $\mathcal{D}_*$  and hence the equilibrium mass flux. One possible resolution of this sensitivity is to note that the similarity structure of a dry convective ABL growing into a uniformly stratified fluid which results in the closure assumption  $\mathcal{B}_- = -\kappa\mathcal{B}$  also predicts

$$\Delta_+ b = N_c^2 h \left( \frac{\kappa}{2\kappa + 1} \right) \quad (71)$$

where  $N_c^2$  is the Brunt–Väisälä frequency in the cloud layer. For a moist adiabatic lapse rate of  $d\theta_v/dz$  of 5 K  $\text{km}^{-1}$  this corresponds to  $\Delta_+\theta_v = (\theta_{00}/g)\Delta_+b \approx 0.36$  K for a sub-cloud layer of 500 m and a moist adiabatic cloud layer ( $N_c^2 = 1.6^{-4} \text{ s}^{-2}$ ). Given  $\Delta_+b$  one can then solve for  $\beta_+$ . Note that from (70), in the limit of  $E \gg \mathcal{D}$ , and with  $w_*$  given following (30) this constraint implies that

$$\mathcal{A} = \frac{2\kappa + 1}{Ri} \quad \text{where} \quad Ri \equiv \frac{h^2 N_c^2}{w_*^2}, \quad (72)$$

is a bulk Richardson number. For typical parameter values this yields values of  $\mathcal{A}$  of about 2%, which is reasonable based on past studies. Preliminary tests of this idea are promising, but it remains to be evaluated more carefully.

## 6 Discussion

In this section we first reflect on our previous results. This discussion is followed by an exploration of some possible extensions to the bulk approach – first to regions of deep convection in Sect. 6.1 and then to incorporate a representation of the winds in Sect. 6.2. We conclude with a brief discussion of regimes which are less obviously representable in terms of these ideas in Sect. 6.3.

For the purposes of diagnostic studies, or simple thermodynamic models of the tropical atmosphere, coupling simple equilibria of the stratocumulus limit with the trade-wind equilibria of the Betts and Ridgway model (Sect. 5) seems like an attractive approach. In this context  $h$  consistently represents the cloud top, or inversion, and hence the two approaches have a compatible mass budget. A further point of continuity is that stratocumulus are thought to decouple precisely when their cloud-base buoyancy flux matches that used to close bulk models of the trade-wind ABL. This fact could guide the choice of  $\beta_-$  to match the representation of the trade-wind layer mass budget with that for stratocumulus. One avenue for future exploration would be to explore such matching in the context of the existing climatological boundary forcings (such as provided by modern reanalysis) and realistic representations of radiative forcings. In so doing it would seem worthwhile to incorporate more-sophisticated representations of partial cloudiness. In this respect the random mixing-line model developed by Park [31] might be a promising approach.

For the purposes of defining a shallow ABL for inclusion in dynamic models it probably makes more sense to couple the sub-cloud model of Sect. 5.2 with the stratocumulus model of Sect. 4. Here, the mass budgets of the two layers are not strictly compatible, with  $h$  formally including a thin cloud layer for the stratocumulus limit, and excluding the cloud layer in the sub-cloud layer limit. So while the matching condition at the transition point does maintain continuity in the sub-cloud buoyancy flux, i.e., sub-cloud solutions are sought when stratocumulus solutions predict  $\mathcal{B}_\eta \geq -\kappa \mathcal{B}_0$ , this provides little guidance as to what to do with  $h$  at the transition point. One possibility is to accommodate the transition through the use of the cloud fraction parameterization in the mass flux. Deep within the trade-wind regimes the parameterization proposed by Neggers et al. [29] acts simply to keep  $h$  near the  $\eta$  and for all practical purposes one might be able to model it as simply

$$\mathcal{A} = \text{Erf} \left( \frac{h - \eta}{\sigma_h} \right) \quad (73)$$

where  $\sigma_h$  is a prescribed length-scale (which could be a function of state) and Erf denotes the error function. In this model  $\mathcal{A}$  increases as  $h/\sigma_h$  becomes large relative to  $\eta/\sigma_h$ , thereby helping to keep  $h$  near  $\eta$ , by venting the ABL if  $h$  becomes too large. In this context further limiting vented cloud fraction as a function of the entrainment coefficient ( $\alpha$ ) could help provide a smooth and physically plausible transition of  $h$ .

As another alternative, we note that when  $\Delta(s + Lq) < 0$  vented cloud water can efficiently cool the air above the ABL thus promoting the development and growth of the trade-wind layer through the injection of liquid water by a venting cloud mass [35]. Roughly speaking  $\Delta(s + Lq)$  transitions from modest positive values over the cold subtropical oceans, to large negative values as one moves over warmer waters. In this respect one could also explore using this (the moist static energy) limit as a basis for further modulating the ventilating cloud fraction in bulk models of the sub-cloud layer as a means of enforcing continuity between the trade-wind and stratocumulus regimes. A variant of this approach, often associated with the idea of cloud-top entrainment instability [13, 32], is already used in one class of general circulation models and appears effective on climatological scales irrespective of whether or not such conditions are associated with the dessication of the stratocumulus layer on the timescales of large eddies in the ABL.

## 6.1 Deep convection

As discussed above, the principal motivation for using of the sub-cloud layer as a basis for a bulk description of the boundary layer is to facilitate coupling to nearby regions of moist convection. Indeed, a variant of the sub-cloud model discussed in Sect. 5.2 is the basis for several descriptions of deep convection [14, 34]. In the deep-convective limit the only change to the equations is that precipitation,  $\Delta F_q$ , is no longer negligible and the mass flux description:

$$M \Delta_+ \phi = -\overline{w' \phi'}_+ \quad (74)$$

ceases to be adequate as it fails to account for convective downdrafts. These downdrafts act to transport air with free-tropospheric properties into the ABL, acting to homogenize the two layers. They are often incorporated by a two-draft model of convective activity, such that

$$\overline{w' \phi'}_+ = m_u (\widehat{\phi} - \phi_+) - m_d (\phi_f - \phi_+), \quad (75)$$

where  $m_u > 0$  is an updraft mass flux and  $m_d > 0$  is a downdraft mass flux, so that the net mass flux out of the ABL is  $M = m_u - m_d$ . If, following Raymond [34], we assume  $m_d = \alpha_m m_u$  with  $0 \leq \alpha_m < 1$ , and use the cloud model (61) then

$$-\overline{w' \phi'}_+ = M \Delta_+ \phi + M \frac{\alpha_m}{1 - \alpha_m} (\phi_f - \widehat{\phi}). \quad (76)$$

The second term on the RHS amounts to an additional source term in the  $\phi$  equations. It acts to relax  $\widehat{\phi}$  to  $\phi_f$  on the timescale  $h/m_d = h(1 - \alpha_m)/(\alpha_m M)$  and, as expected, vanishes for zero downdraft mass flux ( $\alpha_m = 0$ ). In equilibrium the efficacy of this term is less substantial than one might imagine at a first glance. Because an increased downdraft mass flux corresponds to less entrainment, one can think of the fraction  $m_d/E$  of the entrainment flux  $E(\widehat{\phi} - \phi_+)$  being replaced by a flux of  $E(\widehat{\phi} - \phi_f)$ . These will differ insofar as  $\phi_f \neq \phi$ . In the context of our mixing-line model of the cloud layer, this difference is measured by  $\beta_+$ , and matters only in so far as downdrafts are active, i.e.,  $\alpha_m > 0$ . The effects of the downdrafts are perhaps best illustrated from the nature of the equilibrium solutions themselves, although one could question the relevance of such solutions to deep convection which tends to be decidedly more transient. Substituting from above yields:

$$h_\infty = \frac{E - M}{\mathcal{D}}, \quad (77)$$

$$\widehat{s}_\infty = \frac{V s_0 + \tilde{E} s_f - \Delta F_s}{V + \tilde{E}}, \quad \text{and} \quad (78)$$

$$\widehat{q}_\infty = \frac{V q_0 + \tilde{E} q_f - h \widehat{\mathbf{u}} \cdot \nabla q}{V + \tilde{E}}. \quad (79)$$

The key difference between the above equilibria, and those for solutions without downdrafts (e.g., 66–67) is that in the thermodynamic budgets  $\beta_+ E$  has been replaced by an effective entrainment velocity defined as:

$$\tilde{E} \equiv \beta_+ E + M \frac{\alpha_m}{1 - \alpha_m}. \quad (80)$$

Because in convective regions  $E_\infty \approx M_\infty$  this amounts to enhancing entrainment in this equilibrium by the factor  $1 + \alpha_m (\beta_+^{-1} - 1)$ . Thus as  $\beta_+ \rightarrow 1$  the effect of the downdraft term goes to zero. Physically this is because downdrafts act to bring air with the property  $\phi_f$ , rather than  $\phi_+$ , into the sub-cloud layer and for  $\beta_+ = 1$ ,  $\phi_+ = \phi_f$ . In this sense  $\alpha$  measures the degree to which the cloud-layer buffers the sub-cloud layer from the free troposphere, thereby allowing the two layers to decouple and differentiate themselves from one another. In the deep convective limit, when  $\alpha_m$  is large, the sub-cloud layer very effectively feels the properties of the free troposphere.

Some points worth noting from the above analysis are: (1) equilibria are permitted in regions where  $\mathcal{D} < 0$ , they simply require that  $M > E$ ; (2) the solutions above are naturally continuous with those for regions of shallow convection, with  $\alpha_m$  essentially measuring the amount of deep convection; (3) although the focus on the sub-cloud layer for regions of shallow or deep convection would seem to avoid the problem of modeling the cloud layer, the cloud model is effectively specified by the parameters  $\beta_+$ ,  $\alpha_m$  and the height  $z_f$  chosen

for the determination of  $s_f$ . Moreover, it is reasonable to expect these parameters not to be independent of one another. For instance as the cloud layer and the free troposphere become less differentiated deeper convection may ensue and  $\beta_+$  may be expected to increase (so as to preserve a constant  $\Delta_+ b$  at cloud base), along with  $\alpha_m$  and  $z_f$ .

## 6.2 Momentum considerations

Until now we have limited our discussion exclusively to the thermodynamic state of the ABL. Its dynamic state, as represented by  $\hat{\mathbf{u}}$  is also interesting. Not only is it fundamental in determining the surface fluxes, and ocean coupling, but it also determines areas of convergence and divergence, which in turn help determine the types of ABL equilibria one may expect [20]. The concepts discussed above are, however, also very relevant to a treatment of low-level momentum, for which the bulk equations become:

$$h \frac{D\hat{\mathbf{u}}}{Dt} - \Delta_+ \mathbf{u} \left[ \frac{Dh}{Dt} + \mathcal{D}h \right] + hf \mathbf{k} \times \hat{\mathbf{u}} = -\frac{h}{\rho_0} [\nabla \hat{p} - p_+ \nabla \ln h] - \overline{w' \mathbf{u}'_+} + V \Delta_0 \hat{\mathbf{u}}, \quad (81)$$

where  $f$  is an inverse timescale which meters the Coriolis force,  $\mathbf{k}$  is the unit vector pointing upwards, and  $p$  is the pressure. Neglecting the  $\ln h$  term on the RHS and modeling the momentum flux out of the ABL as if momentum were a passive scalar (and hence well represented by the mass-flux approach described above) (81) reduces to

$$h \frac{D\hat{\mathbf{u}}}{Dt} + hf \mathbf{k} \times \hat{\mathbf{u}} = -\frac{h}{\rho_0} \nabla \hat{p} + E \Delta_+ \hat{\mathbf{u}} + V \Delta_0 \hat{\mathbf{u}}, \quad (82)$$

which is similar to the bulk equation for thermodynamic quantities, except for the appearance of the Coriolis term and the pressure gradient (which depends on the state of the layer) as a source term. The ability of steady states of this equation, for a fixed  $h = 500$  m and  $E = 0.01 \text{ m s}^{-1}$  were shown to be a reasonable description of the relationship amongst surface pressure, winds, and the geographic variation of  $f$  [45]. More-systematic applications of this approach have also proven useful in describing the pattern of winds over the eastern tropical Pacific [24]. On a more quantitative level it remains unclear as to the extent to which the entrainment flux can be expressed as

$$E \Delta_+ \mathbf{u} = \Delta_+ \mathbf{u} \left[ \frac{Dh}{Dt} + \mathcal{D}h + M \right] \approx \Delta_+ \mathbf{u} \left[ \frac{Dh}{Dt} + \mathcal{D}h \right] - \overline{w' \mathbf{u}'_+}, \quad (83)$$

where we have assumed that the last term on the RHS behaves as a mass flux following (13), e.g.,  $M \Delta_+ \mathbf{u} = -\overline{w' \mathbf{u}'_+}$ . Because  $\mathbf{u}'/\hat{\mathbf{u}}$  is much closer to unity than either  $s'/\hat{s}$  or  $q'/\hat{q}$  the ability of the circulation to organize fluctuations of  $\mathbf{u}$  in correspondence to the convection, even for regions of shallow convection, may critically determine the net momentum transport through the top of the ABL. These issues become even more acute for deep convection for which momentum fluctuations are on the order of the mean wind and both are organized by, and help organize, areas of enhanced convection.

## 6.3 Missing regimes

Our description of bulk representations of atmospheric ABLs is reasonably complete for tropical maritime regions, where the flow tends to be toward warmer water, so that the surface buoyancy flux,  $\mathcal{B}_0$ , is positive and the sub-cloud layer is convective. However some important regimes are less obviously well described by the above approach. These include regions of stable stratification, such as in the equatorial cold-tongue region of the eastern Pacific, and over land at night. In regions of stable stratification, turbulence in the ABL is often the result of intermittent processes aloft (such as jets, breaking gravity waves, etc.). In such circumstances a bulk formulation wherein  $h$  expresses the depth of the wall-bounded turbulent flow is less obviously relevant. Another problematic regime is over land; here the lack of available moisture and low surface conductivities can promote the development of very deep daytime cloud layers across which baroclinic effects are likely to play a greater role.

## 7 Summary and conclusions

We have reviewed the representation of the ABL using bulk theory, focusing on the representation of the thermodynamic state of tropical and subtropical maritime regimes, away from regions of deep convection. Three paradigms were explored in some detail: (1) stratocumulus-topped mixed layers as embodied by the theory first developed by Lilly [19]; (2) the trade-wind boundary layer as represented by the model of Betts and Ridgway [6], and (3) models of the sub-cloud layer such as initially explored by Betts [5] and more recently (in this volume) by Neggers et al. [29]. For all three approaches we show that closure of the bulk budgets of mass, enthalpy and moisture effectively requires the specification of three exchange velocities  $V$ ,  $M$ , and  $E$  defining surface exchange, mass flux out of the ABL and entrainment at the ABL top respectively. To the extent the state of the surface layer can be related to the state of the bulk layer as a whole  $V$  follows relatively straightforwardly from surface-layer similarity theory. For the stratocumulus-topped ABL and the Betts and Ridgway model of the trade-wind layer, the ABL top is identified with the top of the cloud layer, and hence  $M$  is set to zero. Thus all that remains is to specify  $E$ . For the Betts and Ridgway model this is accomplished by assuming a fixed boundary-layer structure and constraining the cloud base fluxes. For the stratocumulus-topped ABL a determination of  $E$  also relies on assumptions about boundary layer structure (typically that it is well mixed) and are an area of active research. Recent proposals however are shown to work reasonably well and when coupled to the bulk theory yield equilibrium solutions which are plausible representations of the observed climatology. Moreover, much of this climatology can be rationalized by yet simpler closures which yield analytic solutions to the bulk equations as a function of prescribed entrainment efficiencies.

Closure of bulk models of just the sub-cloud layer typically involve additional assumptions. Although the cloud layer is not meant to be modeled, its structure must still be assumed so as to relate the state of the atmosphere just above cloud base to its structure above cloud top. Moreover, in addition to modeling  $E$ , a model of the mass flux,  $M$  out of the layer must also be specified. Typically  $E$  is modeled by assuming that cumulus clouds have a small area and do not interact strongly with the turbulence in the sub-cloud layer. In this case  $E$  is given based on similarity relationships developed for dry convective boundary layers growing into layers of uniform stratification. We show that models of  $M$  which principally act to maintain the depth of the ABL at the lifting condensation level produce reasonable equilibria, characterized by a sub-cloud layer whose depth does not, but whose mass fluxes do, depend on how the cloud layer is modeled. A proposal for avoiding this unsatisfactory parameter dependence is to model the buoyancy jump at the top of the sub-cloud layer using relationships valid for the growth of dry convective boundary layers. So doing effectively constrains one's model of the cloud layer and results in explicit predictions of the cloud core mass fraction, namely that this fraction  $\mathcal{A}$  scales as  $(2\kappa + 1)/Ri$  where  $\kappa$  is the entrainment flux ratio (typically 0.2) and  $Ri$  is the bulk Richardson number defined as  $(\eta N/w_*)^2$ , where  $\eta$  is the height of cloud base,  $N$  is the Brunt–Väisälä frequency in the cloud layer and  $w_*$  is the Deardorff velocity scale. For typical values of  $Ri \approx 60$  this yields cloud core fractions of around 2%, similar to those produced by large-eddy simulation.

Means of blending, or matching, the various bulk regimes are also briefly explored. Here we find that the equilibrium solutions of the Betts and Ridgway model correspond to typical entrainment efficiencies that are not incommensurate with those indicative of decoupling for equilibrium solutions of the bulk equations for stratocumulus mixed layer. As a result one fruitful approach to matching these theories may be to model the assumed boundary layer structure as a function of a decoupling parameter, such as the ratio of the cloud base fluxes to the surface fluxes. Likewise, to couple the bulk representation of stratocumulus-topped boundary layers to models of the sub-cloud structure our analysis suggests that relating the mass flux out of the ABL to the decoupling parameter (so that it becomes zero in regions where stratocumulus are expected) might be an effective approach. This latter type of model is also shown to couple naturally to regions of deep convection, and to previous representations of the bulk winds in the ABL. As such it appears to provide the most promising basis for the incorporation of boundary layer concepts into simplified models of tropical dynamics.

**Acknowledgements** This material is based upon work supported by the National Science Foundation under grant nos. ATM-0336849 and ATM-9985413. The Konrad–Zuse Institute für Informationstechnik Berlin (ZIB) and Rupert Klein are thanked for supplying an office and infrastructure support to the author during the period of the writing of this article as well as his numerous constructive comments on a draft version. Constructive comments by Pier Siebesma and an anonymous reviewer are also gratefully acknowledged. The members of the focused research group on tropical convection are thanked for their input, encouragement and numerous discussions which helped stimulate this research. In particular, Adam Sobel's efforts in organizing and leading this group are gratefully acknowledged. Yunyan Zhang and Brian Medeiros are thanked for their help with some of the calculations using the mixed-layer model of stratocumulus, and in particular the drafting of Figs. 3 and 4.



## References

1. Ahlgrim, M., Randall, D.A.: Diagnosing monthly mean boundary layer properties from re-analysis data using a bulk boundary layer model. *J. Atmos. Sci.* **63**, 998–1012 (2006)
2. Albrecht, B.A., Betts, A.K., Schubert, W.H., Cox, S.K.: A model of the thermodynamic structure of the trade-wind boundary layer. Part I: Theoretical formulation and sensitivity tests. *J. Atmos. Sci.* **36**, 90–98 (1979)
3. Arakawa, A., Schubert, W.S.: Interaction of a cumulus cloud ensemble with the large-scale environment. Part I. *J. Atmos. Sci.* **31**, 674–701 (1974)
4. Bellon, G., Stevens, B.: On bulk models of shallow cumulus convection. *J. Atmos. Sci.* **62**, 3286–3302 (2005)
5. Betts, A.K.: Modeling subcloud layer structure and interaction with a shallow cumulus layer. *J. Atmos. Sci.* **33**, 2363–2382 (1976)
6. Betts, A.K., Albrecht, B.A.: Conserved variable analysis of boundary layer thermodynamic structure over the tropical oceans. *J. Atmos. Sci.* **44**, 83–99 (1987)
7. Betts, A.K., Ridgway, W.: Climatic equilibrium of the atmospheric convective boundary layer over a tropical ocean. *J. Atmos. Sci.* **46**, 2621–2641 (1989)
8. Bretherton, C.S.: Understanding Albrecht’s model of trade cumulus cloud fields. *J. Atmos. Sci.* **50**, 2264–2283 (1993)
9. Bretherton, C.S., Wyant, M.C.: Moisture transport, lower tropospheric stability, and decoupling of cloud-topped boundary layers. *J. Atmos. Sci.* **54**, 148–167 (1997)
10. Cuijpers, J., Duynkerke, P.G.: Large-eddy simulation of trade-wind cumulus clouds. *J. Atmos. Sci.* **50**, 3894–3908 (1993)
11. Deardorff, J.W.: Convective velocity and temperature scales for the unstable planetary boundary layer and for Rayleigh convection. *J. Atmos. Sci.* **27**, 1211–1213 (1970)
12. Deardorff, J.W.: Parameterization of the planetary boundary layer for use in general circulation models. *Mon. Wea. Rev.* **100**, 93–106 (1972)
13. Deardorff, J.W.: Cloud top entrainment instability. *J. Atmos. Sci.* **37**, 131–147 (1980)
14. Emanuel, K.A.: The effect of convective response time on WISHE modes. *J. Atmos. Sci.* **50**, 1763–1765 (1993)
15. Fairall, C.W., Bradley, E.F., Hare, J.E., Grachev, A., Edson, J.: Bulk parameterization of air-sea fluxes: Updates and verification for the COARE algorithm. *J. Climate* **16**, 571–591 (2003)
16. Klein, S.A., Hartmann, D.L.: The seasonal cycle of low stratiform clouds. *J. Climate* **6**, 1587–1606 (1993)
17. Kraus, E.B.: The diurnal precipitation change over the sea. *J. Atmos. Sci.* **20**, 551–556 (1963)
18. Lewellen, D.C., Lewellen, W.: Large-eddy boundary layer entrainment. *J. Atmos. Sci.* **55**, 2645–2665 (1998)
19. Lilly, D.K.: Models of cloud topped mixed layers under a strong inversion. *Q. J. R. Meteor. Soc.* **94**, 292–309 (1968)
20. Lindzen, R.S., Nigam, S.: On the role of sea surface temperature gradients in forcing low-level winds and convergence in the tropics. *J. Atmos. Sci.* **44**, 2440–2458 (1987)
21. Lock, A.: The numerical representation of entrainment in parameterizations of boundary layer turbulent mixing. *Mon. Wea. Rev.* **129**, 1148–1163 (2000)
22. Lock, A.P.: The parameterization of entrainment in cloudy boundary layers. *Q. J. R. Meteor. Soc.* **124**, 2729–2753 (1998)
23. Lock, A.P., MacVean, M.K.: A parametrization of entrainment driven by surface heating and cloud-top cooling. *Q. J. R. Meteor. Soc.* **125**, 271–299 (1999)
24. McGauley, M., Zhang, C., Bond, N.A.: Large-scale characteristics of the atmospheric boundary layer in the eastern Pacific cold tongue ITCZ region. *J. Climate* **17**, 3907–3920 (2004)
25. Miller, R.L.: Tropical thermostats and low cloud cover. *J. Climate* **10**, 409–440 (1997)
26. Moeng, C.H.: Entrainment rate, cloud fraction and liquid water path of PBL stratocumulus clouds. *J. Atmos. Sci.* **57**, 3627–3643 (2000)
27. Moeng, C.H., Sullivan, P.P., Stevens, B.: Including radiative effects in an entrainment-rate formula for buoyancy driven PBLs. *J. Atmos. Sci.* **56**, 1031–1049 (1999)
28. Neggers, R.A., Siebesma, A.P., Lenderink, G.: An evaluation of mass flux closures for diurnal cycles of shallow cumulus. *Mon. Wea. Rev.* **132**, 2525–2538 (2004)
29. Neggers, R.A., Stevens, B., Neelin, J.D.: A simple equilibrium model for shallow cumulus topped mixed layers. *Theor. Comput. Fluid Dynam.* (2006) (in press)
30. Nicholls, S., LeMone, M.A.: The fair weather boundary layer in GATE: the relationship of subcloud fluxes and structure to the distribution and enhancement of cumulus cloud. *J. Atmos. Sci.* **37**, 2051–2067 (1980)
31. Park, S., Leovy, C.B., Rozendaal, M.A.: A new heuristic lagrangian marine boundary layer cloud model. *J. Atmos. Sci.* **61**, 3002–3024 (2004)
32. Randall, D.A.: Conditional instability of the first kind upside-down. *J. Atmos. Sci.* **37**, 125–130 (1980)
33. Randall, D.A., Suarez, M.J.: On the dynamics of stratocumulus formation and dissipation. *J. Atmos. Sci.* **41**, 3052–3057 (1984)
34. Raymond, D.J.: Regulation of moist convection over the west Pacific warm pool. *J. Atmos. Sci.* **52**, 3945–3959 (1995)
35. Riehl, H., Yeh, C., Malkus, J.S., LaSeur, N.E.: The North-East Trade of the Pacific Ocean. *Q. J. R. Meteor. Soc.* **77**, 598–626 (1951)
36. Schlichting, H.: *Boundary Layer Theory*, 7th edn. McGraw–Hill, New York (1979)
37. Schubert, W.H., Wakefield, J.S., Steiner, E.J., Cox, S.K.: Marine stratocumulus convection. Part I: Governing equations and horizontally homogeneous solutions. *J. Atmos. Sci.* **36**, 1286–1307 (1979)
38. Schubert, W.H., Wakefield, J.S., Steiner, E.J., Cox, S.K.: Marine stratocumulus convection. Part II: Horizontally inhomogeneous solutions. *J. Atmos. Sci.* **36**, 1308–1324 (1979)
39. Siebesma, A.P.: Shallow convection. In: Plate, E.J., Fedorovich, E.E., Viegas, D.X., Wyngaard, J.C. (eds.) *Buoyant Convection in Geophysical Flows*, C, vol. 513, pp. 441–486. Kluwer, Dordrecht (1998)
40. Siebesma, A.P., Brown, C.S.B.A., Chlond, A., Cuxart, J., Duynkerke, P., Jiang, H., Khairoutdinov, M., Lewellen, D., Moeng, C.H., Sanchez, E., Stevens, B., Stevens, D.E.: A large-eddy simulation study of shallow cumulus convection. *J. Atmos. Sci.* **60**, 1201–1219 (2003)

41. Stevens, B.: Cloud transitions and decoupling in shear-free stratocumulus-topped boundary layers. *Geophys. Res. Lett.* **27**, 2557–2560 (2000)
42. Stevens, B.: Entrainment in stratocumulus mixed layers. *Q. J. R. Meteor. Soc.* **128**, 2663–2690 (2002)
43. Stevens, B., Ackerman, A.A., Albrecht, B.A., Brown, A.R., Chlond, A., Cuxart, J., Duynkerke, P.G., Lewellen, D.C., MacVean, M.K., Neggers, R., Sanchez, E., Siebesma, A.P., Stevens, D.E.: Simulations of trade-wind cumuli under a strong inversion. *J. Atmos. Sci.* **58**, 1870–1891 (2001)
44. Stevens, B., Beljaars, A., Bordoni, S., Holloway, C., Köhler, M., Savic-Jovicic, S.K.V., Zhang, Y.: On the structure of the lower troposphere: July 2001 near 120W and 30N. *Mon. Wea. Rev.* (2006) (in press)
45. Stevens, B., Duan, J., McWilliams, J.C., Münnich, M., Neelin, J.D.: Entrainment, Rayleigh friction and boundary layer winds over the tropical Pacific. *J. Climate* **15**, 30–44 (2002)
46. Stevens, B., Lenschow, D.H., Ian Faloona, C.H.M., Lilly, D.K., Blomquist, B., Vali, G., Bandy, A., Campos, T., Gerber, H., Haimov, S., Morley, B., Thornton, D.: On entrainment in nocturnal marine stratocumulus. *Q. J. R. Meteor. Soc.* **129**, 3469–3492 (2003)
47. Stevens, B., Moeng, C.H., Ackerman, A.S., Bretherton, C.S., Chlond, A., de Roode, S., Edwards, J., Golaz, J.C., Jiang, H., Khairoutdinov, M., Kirkpatrick, M.P., Lewellen, D.C., Lock, A., Müller, F., Stevens, D.E., Whelan, E., Zhu, P.: Evaluation of large-eddy simulations via observations of nocturnal marine stratocumulus. *Mon. Wea. Rev.* **133**, 1443–1462 (2005)
48. Uppala, S.M., Källberg, P.W., Simmons, A.J., Andrae, U., daCosta Bechtold, V., Fiorino, M., Gibson, J.K., Haseler, J., Hernandez, A., Kelly, G.A., Li, X., Onogi, K., Saarinen, S., Sokka, N., Allan, R.P., Anderson, A., Arpe, K., Balmaseda, M.A., Beljaars, A.C.M., van de Berg, L., Bidlot, J., Bormann, N., Caires, S., Dethof, A., Dragasovac, M., Fisher, M., Fuentes, M., Hagemann, S., Holm, E., Hoskings, B., Isaksen, I., Janssen, P.A.E.M., McNally, A.P., Mahfouf, J.F., Jenne, R., Morcrette, J.M., Raynor, N.A., Saunders, R.W., Simon, P., Sterl, A., Trenberth, K.E., Untch, A., Vasiljevic, D., Viterbo, P., Woolen, J.: The ERA-40 re-analysis. *Q. J. R. Meteor. Soc.* **131**, 2961–3012 (2005)
49. Wood, R., Bretherton, C.S.: Boundary layer depth, entrainment and decoupling in the cloud-capped subtropical and tropical marine boundary layer. *J. Climate* **17**, 3576–3588 (2004)
50. Zhang, Y., Stevens, B., Ghil, M.: On the diurnal cycle and susceptibility to aerosol concentration in a stratocumulus-topped mixed layer. *Q. J. R. Meteor. Soc.* **131**, 1567–1584 (2005)